Exp Astron (2012) 33:491–527
DOI 10.1007/s10686-011-9233-6

ORIGINAL ARTICLE

EIDOSCOPE: particle acceleration at plasma boundaries

A. Vaivads · G. Andersson · S. D. Bale · C. M. Cully · J. De Keyser · M. Fujimoto · S. Grahn · S. Haaland · H. Ji · Yu. V. Khotyaintsev · A. Lazarian · B. Lavraud · I. R. Mann · R. Nakamura · T. K. M. Nakamura · Y. Narita · A. Retinò · F. Sahraoui · A. Schekochihin · S. J. Schwartz · I. Shinohara · L. Sorriso-Valvo

Received: 24 February 2011 / Accepted: 10 June 2011 / Published online: 16 July 2011

Abstract We describe the mission concept of how ESA can make a major contribution to the Japanese Canadian multi-spacecraft mission SCOPE by adding one cost-effective spacecraft EIDO (Electron and Ion Dynamics Observatory), which has a comprehensive and optimized plasma payload to address

A. Vaivads (✉) · C. M. Cully · Yu. V. Khotyaintsev
Swedish Institute of Space Physics, Box 537, SE-751 21 Uppsala, Sweden
e-mail: andris@irfu.se

G. Andersson · S. Grahn
Swedish Space Corporation, Stockholm, Sweden

S. D. Bale
Physics Department and Space Sciences Laboratory,
University of California, Berkeley, CA, USA

J. De Keyser
Belgian Institute for Space Aeronomy, Brussels, Belgium

M. Fujimoto · T. K. M. Nakamura · I. Shinohara
Institute of Space and Astronautical Science, JAXA, Tokyo, Japan

S. Haaland
University of Bergen, Bergen, Norway

H. Ji
Princeton Plasma Physics Laboratory, Princeton, NJ, USA

A. Lazarian
Department of Astronomy, University of Wisconsin, Madison, USA

B. Lavraud
Institut de Recherche en Astrophysique et Plantologie,
Universit de Toulouse (UPS), Toulouse, France

the physics of particle acceleration. The combined mission EIDOSCOPE will distinguish amongst and quantify the governing processes of particle acceleration at several important plasma boundaries and their associated boundary layers: collisionless shocks, plasma jet fronts, thin current sheets and turbulent boundary layers. Particle acceleration and associated cross-scale coupling is one of the key outstanding topics to be addressed in the Plasma Universe. The very important science questions that only the combined EIDOSCOPE mission will be able to tackle are: 1) Quantitatively, what are the processes and efficiencies with which both electrons and ions are selectively injected and subsequently accelerated by collisionless shocks? 2) How does small-scale electron and ion acceleration at jet fronts due to kinetic processes couple simultaneously to large scale acceleration due to fluid (MHD) mechanisms? 3) How does multi-scale coupling govern acceleration mechanisms at electron, ion and fluid scales in thin current sheets? 4) How do particle acceleration processes inside turbulent boundary layers depend on turbulence properties at ion/electron scales? EIDO particle instruments are capable of resolving full 3D particle distribution functions in both thermal and suprathermal regimes and at high enough temporal resolution to resolve the relevant scales even in very dynamic plasma processes. The EIDO spin axis is designed to be sun-pointing, allowing EIDO to carry out the most sensitive electric field measurements ever accomplished in the outer magnetosphere. Combined with a nearby SCOPE Far Daughter satellite, EIDO will form a second pair (in addition to SCOPE Mother-Near Daughter) of closely separated satellites that provides the unique capability to measure the 3D electric field with high accuracy and sensitivity. All EIDO instrumentation are state-of-the-art technology with heritage from many recent missions. The EIDOSCOPE orbit will be close to equatorial with

I. R. Mann
University of Alberta, Edmonton, Canada

R. Nakamura
Space Research Institute, Austrian Academy of Sciences, Graz, Austria

Y. Narita
Institute of Geophysics and Extraterrestrial Physics, Braunschweig, Germany

A. Retinò · F. Sahraoui
Laboratoire de Physique des Plasmas (LPP), Observatoire de St Maur,
4, Avenue de Neptune, 94107 St Maur-des-Fossés, France

A. Schekochihin
Rudolf Peierls Centre for Theoretical Physics, University of Oxford, Oxford, UK

S. J. Schwartz
Blackett Laboratory, Imperial College London, London, UK

L. Sorriso-Valvo
CNR-IPCF - Liquid Crystals Laboratory, Ponte P. Bucci 31C, 87036 Rende, Italy

apogee 25-30 RE and perigee 8-10 RE. In the course of one year the orbit will cross all the major plasma boundaries in the outer magnetosphere; bow shock, magnetopause and magnetotail current sheets, jet fronts and turbulent boundary layers. EIDO offers excellent cost/benefits for ESA, as for only a fraction of an M-class mission cost ESA can become an integral part of a major multi-agency L-class level mission that addresses outstanding science questions for the benefit of the European science community.

Keywords Cosmic vision · Particle acceleration · Multi-scale coupling in plasmas · Space plasmas

1 Introduction

Universality of the particle acceleration Most of the visible universe is in the highly ionised plasma state. H. Alfvén even coined the term Plasma Universe [1]. Plasma processes are at work everywhere, from radio galaxy jets and supernova explosions to solar flares and planetary magnetospheres. One of the most important and exciting properties of the Plasma Universe is the explosive behavior of various energy conversion processes. The source energy is accumulated in a large volume. The large-scale plasma motion that is responsible for the energy build-up also creates embedded plasma boundaries inside the energy-storing space. When micro-physics, with much faster time scales, sets in at the boundaries, explosive onsets of an energy conversion process take place. These explosive processes not only simply heat the plasma but lead to charged particle acceleration to well above thermal energies. Understanding particle acceleration mechanisms is of major importance in space science.

Importance of scales Particle acceleration is controlled by electromagnetic field dynamics across fundamental plasma scales: Debye length, electron kinetic, ion kinetic, fluid and system size. The kinetic scales are given by corresponding inertial length or gyroradius scales. The interaction of electrons and ions with electromagnetic fields on all these scales leads to different types of particle acceleration, from the formation of strong beams to the formation of extended suprathermal tails in particle distribution functions. The strongest particle acceleration is produced by electromagnetic fields at the boundaries where the micro-physical processes are operative. The micro-physics, in turn, is driven by the external large-scale dynamics in which the boundary is embedded and the micro-physics can also lead to the changes in the large-scale plasma dynamics. Understanding particle acceleration thus involves identifying the micro-physical agents and elucidating how they are driven and how they interact with the ambient large-scale plasma dynamics. This influence of small scales on larger scales is very evident, e.g. in the context of magnetic reconnection, where a phenomenon occurring in a very

small region deeply impacts the plasma dynamics at the scale of the full magnetosphere.

Space boundaries addressed by EIDOSCOPE The Earth's space environment is determined by the interaction between the solar wind, a supersonic plasma flow originally ejected from the upper atmosphere of the sun, and the terrestrial magnetic field and plasmas confined by that magnetic field. This global solar wind-magnetosphere interaction process creates different plasma boundaries where coupling with large-scale bulk plasma processes and the kinetic processes can be studied in detail. This makes near-Earth space an ideal place to study particle acceleration processes involving different scales. Figure 1 shows the main boundaries and boundary layers that are created in this interaction region around the Earth: the bow shock, at which the supersonic solar wind is decelerated; the magnetosheath, which is a turbulent transition layer; the magnetopause, which is the outer boundary of the magnetosphere. The energy transport/transfer process inside the magnetosphere is driven strongly by the reconnection at the magnetopause and the magnetotail. The magnetotail reconnection creates Earthward plasma jets that interact with the Earth's dipole field and ambient plasma forming another boundary layer: the jet front layer. These are the main plasma boundaries and boundary layers that EIDOSCOPE will observe.

Space as the best in situ laboratory for kinetic scales Critically, most astrophysical plasmas are collisionless, which means that their constituents can be far from thermodynamic equilibrium with each other. The resulting

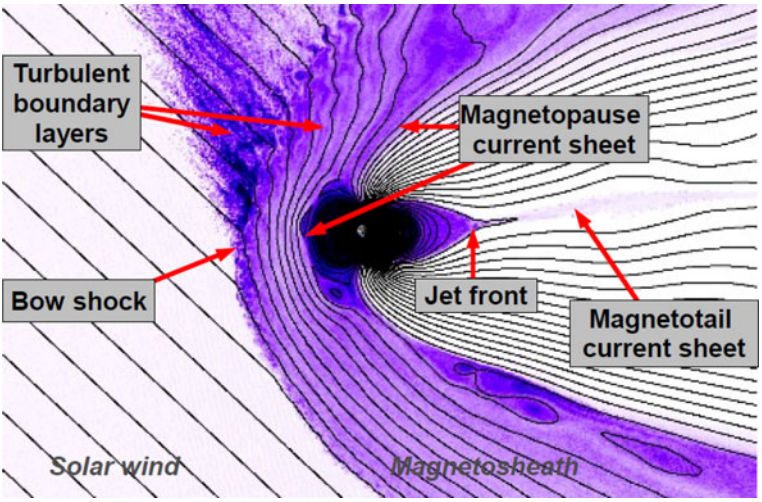

Fig. 1 Typical location of plasma boundaries encountered by EIDOSCOPE. This illustration of the magnetosphere is from a hybrid simulation, courtesy D. Krauss–Varban

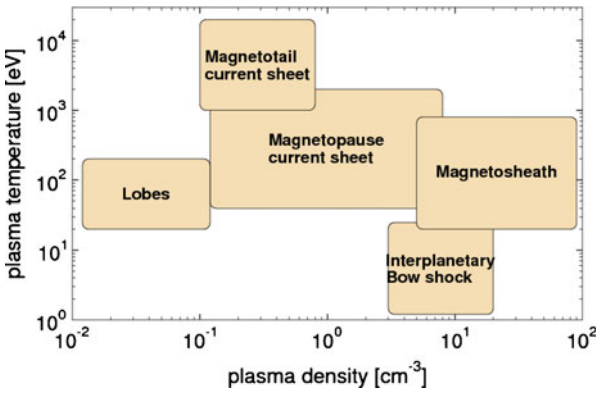

Fig. 2 Typical plasma parameters encountered by EIDOSCOPE. Plasma temperature reflects proton temperature. Electron temperature is usually ∼5 times smaller and heavy ion temperature can be a few times larger than proton temperature

nonlinear dynamics provides diverse mechanisms for momentum and energy flow and redistribution as well as charged particle acceleration. In situ space observations allow detailed observations of those processes down to particle kinetic scales. Simultaneous measurements of particle distribution functions and electromagnetic fields are accessible only in space and are required to address the questions of particle acceleration. Figure 2 shows the wide range of plasma parameters (density and temperature) where particle acceleration can be studied in the outer magnetosphere. The EIDO instruments will be designed such that all this parameter space will be covered. Figure 3 illustrates that despite that the plasma density and magnetic fields in laboratory, space and

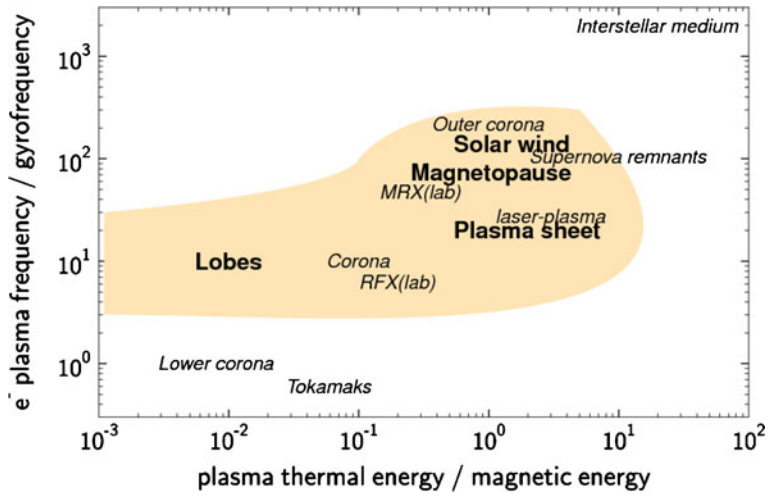

Fig. 3 Typical non-dimensional plasma parameters encountered by EIDOSCOPE compared to laboratory/solar/astrophysical plasma environments. Example laboratory experiments included here are Magnetic Reconnection Experiment or MRX [2], Reversed Field Pinch Experiment or RFX [3] and large tokamaks, e.g. [4]

Table 1 Multi-spacecraft missions in near-Earth space

Mission	Years	Description	European contribution
ISEE-1,2	1977–1987	2 s/c, outer magnetosphere	ESA/NASA mission
DE-1,2	1981–1990	2 s/c, inner magnetosphere	Hardware contribution
AMPTE	1984–1989	3 s/c, outer/inner magnetosphere	UK/German/NASA mission
Cluster	2000–2014	4 s/c, ion/fluid scales	ESA/NASA mission
THEMIS	2007–2009	5 s/c, system scales, substorm onset	Hardware contribution
MMS	2014–	4 s/c, electron scale reconnection	Hardware contribution
SCOPE	2020–	5+ s/c, cross-scale coupling	EIDO

There has been a major European contribution to almost all of those missions

astrophysical plasmas can differ by more than 20 orders or magnitude, when plotted in non-dimensional plasma parameters, those plasmas can be rather similar to each other.

Multi-spacecraft missions Table 1 shows multi-spacecraft missions that have been studying near-Earth space. Each of these missions has had its dedicated goal of scales and corresponding physics topics to be addressed. EIDOSCOPE would be the first dedicated mission to study multi-scale plasma physics.

EIDOSCOPE configurations Figures 4–6 sketch the basic spacecraft configurations during the mission's nominal phase. There are many unique and decisive contributions that EIDO can bring to the SCOPE constellation in studying particle acceleration at plasma boundaries. For example, only EIDOSCOPE(but not SCOPE alone) will allow:

- to quantify at sufficiently high temporal resolution essential plasma particle and field parameters simultaneously on both sides of plasma boundaries,
- to have high precision 3D electric field measurements and resolved electron-scale observations in two spatially separated locations,

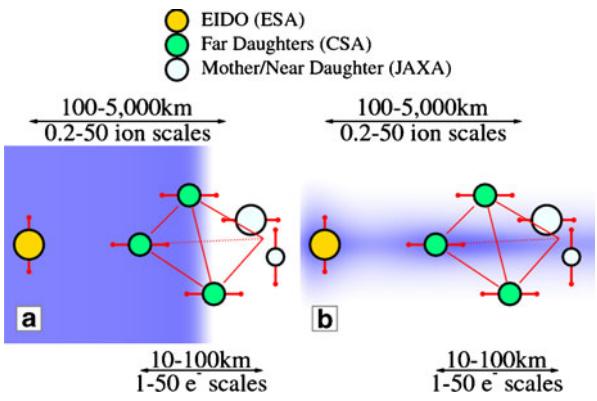

Fig. 4 EIDO configuration 1, the first phase of the mission, illustrating how EIDO will be able to add one more scale (ion/fluid) to EIDOSCOPE. The SCOPE Mother/Near Daughter spacecraft are separated on electron scales. **a** Typical orientation of the bow shock, magnetopause, and jet braking boundaries. **b** Typical orientation of the current sheet found in the magnetotail

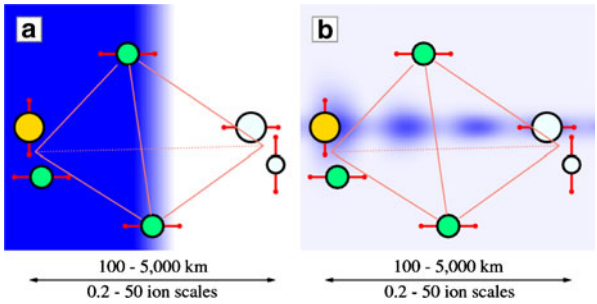

Fig. 5 EIDO configuration 2, the second phase of the mission. EIDO and one SCOPE Far Daughter spacecraft will form a second electron scale pair of spacecraft. In concert with the SCOPE Mother/Near Daughter, this configuration will perform simultaneous dual-spacecraft electron-scale measurements at two locations which are separated by ion or fluid scale distances

– to observe simultaneously on one additional scale enabling detailed studies of multi-scale coupling that are essential for particle acceleration,
– to measure key properties of the boundaries such as curvature and dynamics.

The combined EIDOSCOPE mission, in comparison to SCOPE alone, will be able to address in a much more conclusive way the key science questions of particle acceleration at plasma boundaries that represent the cutting edge science topic for plasma astrophysics.

2 Science

The science requirements on EIDO payload are specified in Table 2. The rest of the section addresses in detail the science questions that have lead to those requirements.

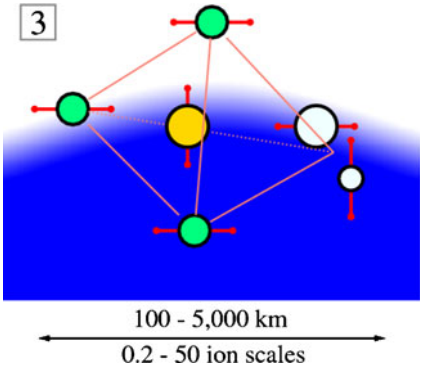

Fig. 6 EIDO configuration 3, the third phase and possibly the extension phase of the mission. The configuration shown can be used to estimate arbitrary boundary curvature, acceleration, and deceleration

Science question I. Collisionless shocks *Quantitatively, what are the processes and efficiencies with which both electrons and ions are selectively injected and subsequently accelerated by collisionless shocks?*

Collisionless plasma shocks are some of the most spectacular, visually-striking and energetic phenomena in the Universe. Generated by supernovae, stellar winds, or the rapid motion of objects such as neutron stars, they have a number of important effects. A primary accelerator for galactic cosmic rays is widely believed to be shocks driven by supernova remnants, where Mach numbers can reach 400 or more. A key, yet unknown, ingredient in this process is the injection of suprathermal particles into the acceleration mechanism. That injection occurs over a thin "sub-shock" region at which

Table 2 Science requirements on EIDO payload

Science requirement	Comment
R1 E, B fields	E, B fields should be measured with sufficient temporal resolution to resolve the smallest electron scales and for E field also the smallest Debye length scales.
R2 E, B field sensitivity	E, B fields should be measured with sufficient sensitivity to have the noise floor below the typical lowest wave amplitudes observed at least down to sub-ion scales.
R3 E, B field accuracy	E, B fields should be measured with sufficient accuracy, 0.1 mV/m and 0.1 nT. (This would correspond to ∼10 km/s accuracy of ExB-drifts across boundaries for ambient B=10 nT).
R4 3D E field	3D electric field should be continuously measured across boundaries with at least sub-ion scale resolution having the same sensitivity (R2) and accuracy (R3) requirements on the third electric field component but only in a combination with a nearby spacecraft.
R5 thermal electrons/ions	Thermal electron/ion 3D distribution functions should be resolved with sufficient temporal resolution to resolve respectively electron/ion characteristic scales.
R6 energetic electrons/ions	Suprathermal and energetic electron/ion 3D distribution functions up to at least 500 keV should be measured at least on ion scales.
R7 thermal ion composition	Thermal ion mass-resolved 3D distribution functions of major ion species H^+, He^{++}, He^+ and O^+ should be measured at least on the characteristic scale of respective ions.
R8 energetic ion composition	Mass resolved 3D distribution function at least up to 500 keV of major ion species H^+ and O^+ should be resolved on their respective scale.
R9 phase speeds	EIDO alone and/or in combination with other satellites should resolve typical phase speeds comparable to typical electron thermal speeds and/or electron Alfvén velocities and/or whistler phase speed, ≤20,000 km/s.
R10 plasma density resolution	To measure the plasma density fluctuations and density gradients down to electron scales with precision better than ∼10%.

the final bulk deceleration, corresponding to Mach numbers in the range 5–40, takes place. The interaction of the fast-moving solar wind with the Earth's magnetosphere results in a bow shock. While the size, curvature and incident flow speed at the terrestrial bow shock limit its ability to accelerate particles to the highest energies, Mach numbers can reach 20, comparable to the sub-shock regions within supernova shocks that fuel the injection of suprathermal particles for the subsequent Fermi acceleration mechanism. The age, large scale, and strength of interplanetary shocks provide access to a wider range of parameters over which to explore the relative efficiencies of ion and electron acceleration. Thus high-resolution observations at interplanetary shocks offer breakthroughs in understanding what factors control the relative efficiencies of electron and ion acceleration.

A knowledge of the intricate feedback between very fine scale electric field structures and ion dynamics, and the resulting variability in the shock profile and structure, will lead to a definitive solution to the "injection problem" that is at the heart of shock acceleration as invoked for cosmic-ray production. In order to quantify the effects of shock ripples, measurements are required of gradients of the shock surface at fluid scales; of ion distribution variations around and within the ripples, with variations on the scale of an ion gyroradius; and of electron heating and acceleration at the smallest scales. The origin and evolution of the cycle of turbulence and particle distributions need to be explored by measurements at the disparate scales. The coupling of such features to larger-scale diffusive (Fermi) acceleration from initial injection to power-law energy spectrum remains an observational challenge that only EIDOSCOPE can address, particularly during the first phase of the mission (see Fig. 4).

The numerical results in Fig. 7, for example, suggest that the shock surface is rippled by local ion and current instabilities. The observational properties of these ripples, e.g., amplitude and wavelength, are unknown. The ripples provide time-varying fields which can trap some particles, enabling them to "surf" the shock front and systematically pick up energy from the large-scale motional electric field. Such surfing is potentially important for both ion and electron acceleration.

Science question II. Jet fronts *How does local electron and ion acceleration at jet fronts due to kinetic processes couple simultaneously to large scale acceleration due to fluid (MHD) mechanisms?*

High speed plasma flows, commonly referred to as jets, are ubiquitous in plasma environments. Jets are observed in laboratory devices [6], in the magnetospheres of Earth [7, 8] and other planets, in the solar corona [9] and chromosphere [10], and in most classes of compact astrophysical objects that rotate rapidly and/or accrete matter from their surroundings, such as proto-stars [11] or supermassive black holes [12].

A fundamental aspect of jet physics, that is very important for particle acceleration, concerns the way jets propagate and interact with the ambient

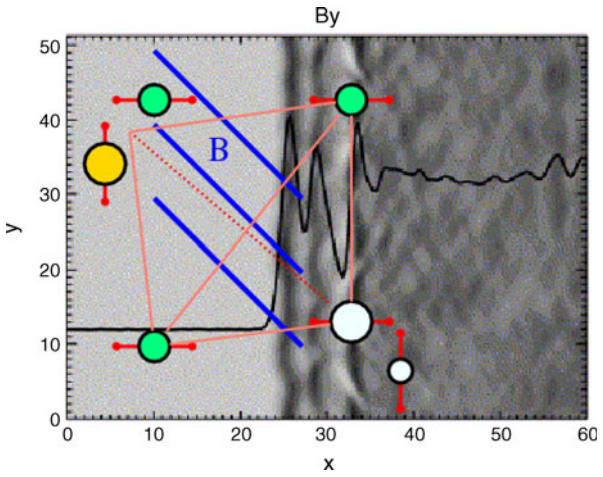

Fig. 7 Two-dimensional magnetic field maps of a "rippled" simulated shock overlain with the average shock profile (from [15]). Axes are in units of the proton inertial length $c/\omega pi$, which is an order of magnitude smaller than the ion gyration in the magnetic field. These ripples influence the ion dynamics/reflection, and serve as sites of possible electron trapping and acceleration [5]. Overlain is the EIDOSCOPE configuration showing the ability to measure 3D electric fields and gradients both along the magnetic field (*blue lines*) and along the shock surface

medium and obstacles. Such interaction leads to the deceleration and eventually the braking of jets resulting in the dissipation of much of their kinetic energy into electromagnetic energy. This leads to the creation of strong electric fields causing strong particle heating and acceleration. An example is the hard X-ray emission from loop-top sources during solar flares, that is believed to be produced by energetic electrons accelerated when the reconnection jet hits the dense loop plasma in front of it [13].

In situ measurements in the Earth's magnetosphere, particularly in the magnetotail where the magnetic field topology is often similar to that during solar flares, can play an important role in the identification of the different particle acceleration mechanisms. Transient and localized plasma jets play a major role in the mass, energy and magnetic flux transport in the Earth's magnetotail [7, 14]. EIDOSCOPE will be able to address the particle acceleration both for acceleration at propagating jet fronts and for acceleration around the dipole obstacle, where jets eventually brake (jet braking region), and will establish the connection between these two cases. Such jets are most likely created by reconnection in the magnetotail current sheet, although other generation mechanisms such as current disruption may be important [15]. The link between particle acceleration at jet fronts in the jet braking region and the injection process into the inner magnetosphere is not yet understood.

At fluid spatial and temporal scales particle acceleration is produced by adiabatic betatron and Fermi acceleration mechanisms within large-scale magnetic flux tubes moving with the jets. However, at smaller scales, large

enhancements of ion and electron fluxes up to many 100s keV occur within jet fronts [16, 17], mostly due to non-adiabatic mechanisms. Observations indicate that strong electric fields and waves therein can efficiently trap and accelerate both ions and electrons, as shown in the bottom right panel in Fig. 8. For this case, the size of the front layer is between ion and electron scales and acceleration mechanisms for protons and electrons are different, as indicated by the difference in their pitch-angle distributions.

This example singles out the important multi-scale aspects of acceleration at jet fronts. Determining accurately the spatial scale and the orientation of the front layer at ion/sub-ion scales is essential for understanding the acceleration and scattering processes since ions and electrons behave differently across the thin front. Also, the maximum energy gain that can be obtained from

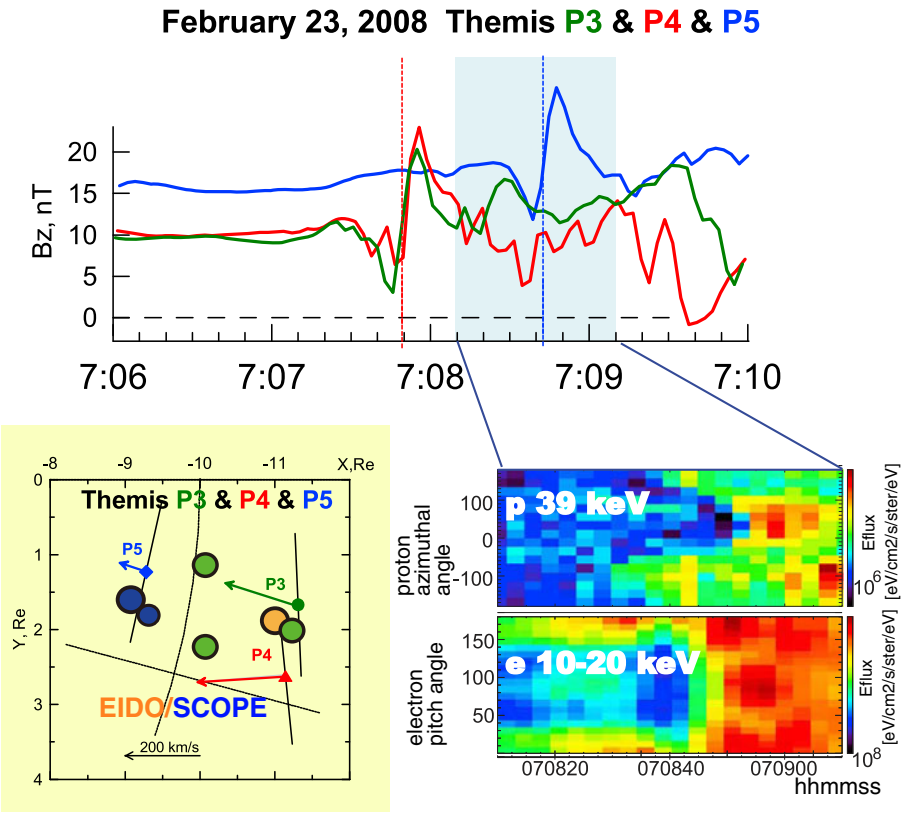

Fig. 8 THEMIS three inner spacecraft observations of a jet braking region [16]. Enhanced energetic particle flux is identified at the boundary within jet front where sharp changes in Bz occur. Energetic ions having larger gyroradii respond differently than the electrons due to the finite thickness of the boundary. The three spacecraft observed a similar front, but the background field increases as the distance decreases from the Earth. In order to understand the acceleration process, both the large-scale change and the local structure of the boundary needs to be captured. A possible configuration of EIDOSCOPE is overlaid in the *left panel*

acceleration by the motional electric field along the jet front depends on its lateral extension (much larger than its thickness). Hence multi-spacecraft observations at several ion scales are necessary to infer the lateral size of the jet front and to eventually establish the efficiency of the direct electric field acceleration in comparison to e.g. wave turbulent acceleration. Simultaneously, determining large-scale gradients in the ambient magnetic field is crucial to determine the effect of the adiabatic acceleration. Since the newly accelerated energetic particles can rapidly drift away from the acceleration site, it is essential to monitor the particle distributions at multiple scales to judge if the observed pitch-angle distribution is due to local acceleration or is an effect of the drift. This requires monitoring the structure/evolution of the jet front through meauserements by spacecraft separated by fluid scale, i.e. several 1000s km.

Science question III. Thin current sheets *How does multi-scale coupling govern acceleration mechanisms at electron and ion/fluid scales in thin current sheets?*

Electric currents in astrophysical plasmas are very often concentrated in thin sheets. In most cases current sheets are driven by the large-scale dynamics of magnetic fields and plasma. Examples are current sheets in the solar corona, created by photospheric flux tubes motion and separating plasma of similar properties, and the terrestrial magnetopause, forming upon interaction of plasmas with different origin and therefore different properties (solar and magnetospheric). Current sheets can be very extended, that is, their extension can be comparable with the typical scale of the system. Examples are current sheets in the solar corona [18], in the quiet solar wind [19] and the spectacular heliospheric current sheet, which threads the entire heliosphere until it interacts with the termination shock and accelerate particles to high energies [20]. On the other hand, current sheets can have an extension that is much smaller than the scale of the system. For example, small-scale current sheets can spontaneously form in a turbulent environment and fill large volumes. Examples of small-scale current sheets are found in the near-Earth space both at ion [21, 22] and electron [23] scales. Other examples are turbulent current sheets in accretion disks or in the solar corona and the solar wind [24, 25]. Electron scale current sheets are also studied extensively in laboratory plasmas such as in Magnetic Reconnection Experiment or MRX [26]. Current sheets are places where free energy contained in plasma can be efficiently released into particle acceleration, via a number or mechanisms such as magnetic reconnection, Kelvin-Helmholtz instability and wave-particle interactions.

Figure 9a shows one example a numerical simulation of electron acceleration in a thin current sheet with developed magnetic islands [27]. A small number of electrons (shown by black dots) are accelerated to relativistic energies at the reconnection site by the inductive electric field (coloured background) arising from the islands growth and coalescence. Simulations also suggest that particle acceleration strongly depends on the guide field

(magnetic field component along the current direction). Figure 9b shows a 3D simulation of a thin current sheet with guide field and shows the geometry of the magnetic islands/flux-ropes [28]. Numerical modelling indicate that reconnecting current sheets form magnetic islands of various sizes that develop and coalesce both in the solar and magnetospheric environments [29–31]. A multi-island environment is very dynamic. Both parallel electric fields at reconnection sites, inductive electric fields associated with rapid changes of the magnetic field, and betatron and Fermi acceleration in contracting islands may drive electron acceleration [27, 32]. The specific acceleration processes at work depend on the island size, yet acceleration may occur at all stages of island formation. Multi-scale island formation remains poorly explored. Answering how particles are accelerated in such scenario requires simultaneous multi-scale observations where both magnetic island scales (several ion scales up to fluid scales) and scales below an ion scale (to resolve localized electron acceleration) have to be carried out simultaneously. Observations of small-scale islands at the magnetopause and magnetotail current sheets have been provided recently [33, 34], including the observation of island coalescence [35], which was largely based on the comparison between data and simulations. These studies have highlighted the limitations of current spacecraft measurements since these can only target the dynamics of island formation at a single scale characteristic of the spacecraft separation. Furthermore, instruments lack the high temporal resolution that is required to resolve thermal and suprathermal particle dynamics within islands.

Science question IV. Turbulent boundary layers *How do particle acceleration processes inside turbulent boundary layers depend on turbulence properties at ion/electron scales?*

The Plasma Universe is often in a turbulent state. The plasma dynamics is strongly nonlinear resulting in unordered, chaotic fluctuations of plasma velocities, densities, electric and magnetic fields. Turbulence is the natural, universal process through which energy is transfered from large-scale sources to smaller scales due to nonlinear plasma interactions generating fluctuations at smaller and smaller scales. At the smallest scales dissipation mechanisms become efficient and the energy is transferred into particle heating and acceleration. The nature of turbulent energy transfer through scales is still not fully understood, and represents one of the most intriguing problems of modern physics [36, 37]. Turbulence is thought to play an important role in many astrophysical environments, as for example in the interstellar [38] and interplanetary media [39], as well as in stellar convective motions [40].

Turbulence is mostly characterized by inhomogeneity, anisotropy, and intermittency. These are often due to the finite size of the systems, or the properties and geometry of the energy injection mechanisms, or anisotropic force terms such as gravity, or the presence of boundaries. Turbulent fluctuations of space plasmas are intrinsically 3D, but due to the presence of an ambient magnetic field they tend to be strongly anisotropic. The anisotropy of fluctuations has

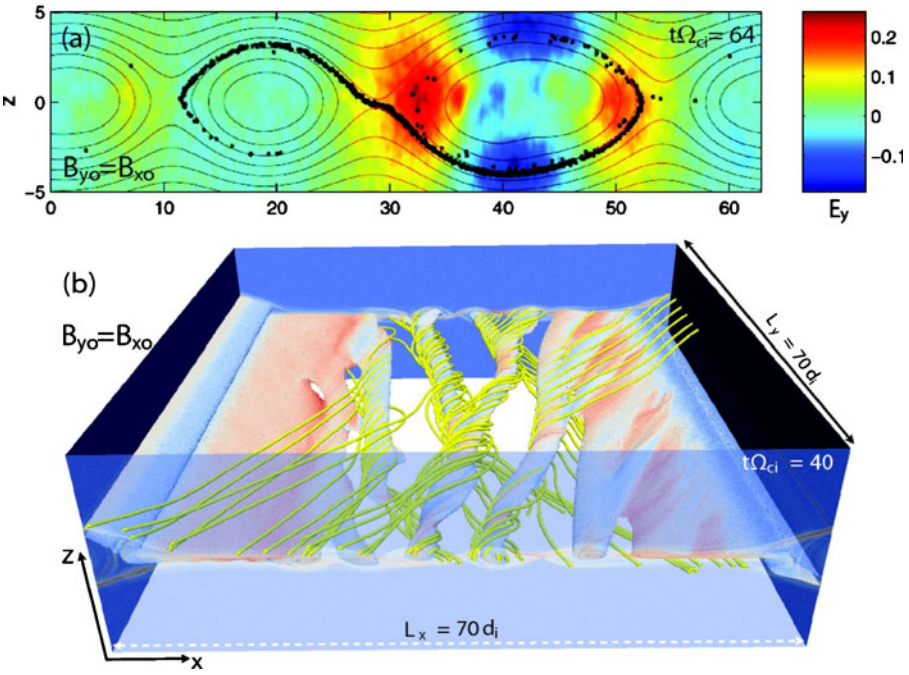

Fig. 9 Dynamic magnetic islands within thin current sheets. **a** Electric fields and acceleration of energetic electrons [27]. **b** Formation of islands/flux-ropes in a 3D simulation with a guide field [28]

been quantified at small scales, showing lack of universality [39, 41]. In wave vector space, scales perpendicular to the ambient magnetic field are shorter than parallel ones [42]. This behaviour has been shown to be scale dependent [43]. Study of cosmic ray transport suggests that the perpendicular turbulence geometry must play a dominant role to account for the long mean free paths of cosmic rays [44]. On the other hand, recent Cluster observations show that anisotropy is different from region to region [45]. Understanding how turbulence and the resulting particle acceleration are affected by presence of boundaries, as well as by the anisotropy and inhomogeneity is a key issue that is far from being properly understood.

Figure 10 displays the distribution of currents on ion to electron scales obtained from an electron-magnetohydrodynamics numerical simulation. Full particle 3D simulations are needed in order to resolve the details of particle acceleration at such electron-scale current sheets. At present, such simulations can accommodate only a very limited range of scales, and simultaneous resolution of MHD and electron scales in 3D is not possible. Simultaneous multi-scale observations of turbulent electric and magnetic fields and particle distributions are crucial to understand the conversion of turbulent energy into ion and electron heating and particle acceleration.

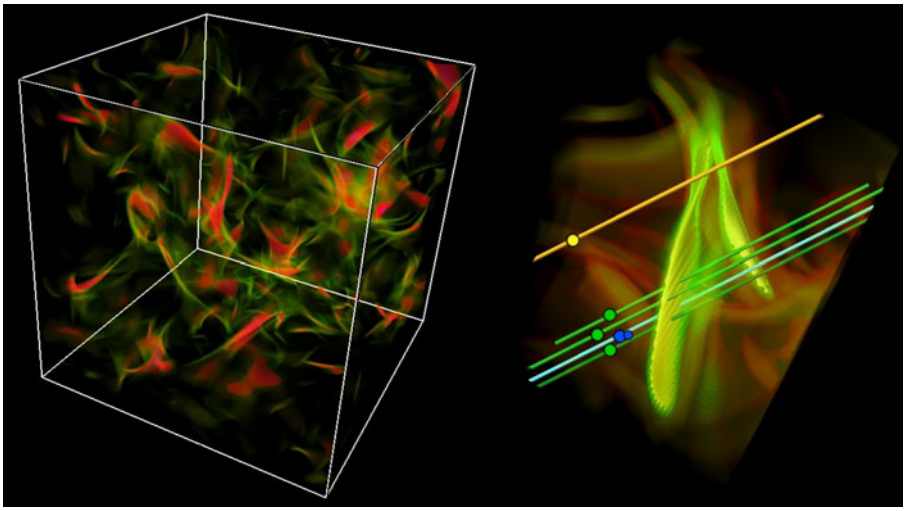

Fig. 10 3D simulation of Hall MHD turbulence reveals that plasmas are spatially localized into thin current sheets and eddies (*left side*) [46]. Multi-point measurements of EIDOSCOPE are essential to discriminate between spatial and temporal variations of electric and magnetic fields, and to describe the plasma properties surrounding the current sheets. A possible trajectory of the spacecraft fleet across one current sheet is shown (*right side*). Courtesy S. Servidio

At small scales, the importance of multi-scale measurements becomes evident. On small scales, temporal variations no longer reflect convected spatial variations and the electric and magnetic fields must be measured with the caharacteristic spatial resolution of local processes. The electric field must be measured in three dimensions (i.e., three components) to distinguish between distinct wave-particle interaction mechanisms, *e.g.*: particle acceleration associated with electric fields parallel to the mean magnetic field (Landau resonance), and acceleration by rotating perpendicular electric fields (cyclotron resonance). The concept of EIDOSCOPE providing 3D electric field measurements at two spatial points is essential for their purpose (Configuration 2). This will give two pairs of measurements of the electric field components, in the same direction, providing small scale spatial resolution in one direction. Likewise, since ion heating is essentially a kinetic process, two point small-scale measurements of ion distribution functions (at different energies) will be employed to determine the solar wind heating and particle acceleration mechanisms.

Multi-point Cluster observations [47] have recently shown that turbulence anisotropy exists on sub-ion scales [48] bringing new questions on the nature of the fluctuations which are hard to answer only with magnetic field measurements as previously done on larger scales. Knowledge of electric field and particle distribution functions at sub-ion scales is needed for satisfactory analysis of the problem. It is important to understand what exactly the anisotropic fluctuations look like in 3D. Moreover, for problems such

as particle acceleration, it is crucial to quantify the relative scalings in the parallel and perpendicular direction, and to compare them with theoretical and numerical results [49].

3 Multi-spacecraft boundary methods applicable for EIDOSCOPE science

Single scale methods To meet the proposed EIDOSCOPE science goals requires not only the accurate measurements of the parameters but also the dedicated analysis of the obtained sets of parameters from multi-point observations. Table 3 gives an overview of some of the most commonly used single and multi-spacecraft methods, their capabilities and required input data. Studies based on four spacecraft have provided a wealth of new insight about plasma structures in space and they have also led to a revival and a verification of many single spacecraft methods. Without further assumptions and constraints, four is the minimum number of measurements to resolve fully spatio-temporal ambiguities over a single scale, but with some a priori knowledge about a boundary, the same techniques can also be applied with two-point (pair) or three-point measurements.

Multi-scale methods For a deeper understanding of acceleration processes at plasma boundaries, simultaneous observations on several scales are required. EIDOSCOPE, with its 6 spacecraft, will add this new multi-scale dimension combining different boundary layer analysis techniques at different scales, as can be seen in Table 4. Increasing the number of the spatial scales of interest, however, does not necessarily mean the necessity of 4-point measurements at each scale. Planarity and/or stationarity condition(s) are often fulfilled for the timescale of interest at the plasma boundaries where EIDOSCOPE observations take place, at least for certain scales, so that a 3D (4-point) measurement is not required for such scales to characterize the process. More sophisticated data analysis methods that exploit physical or geometrical considerations can reduce the required number of points or can be used to verify some of the assumptions, such as planarity, acceleration, or time-stationarity of the boundary. In particular, Configuration 3 with a properly positioned EIDOSCOPE can specifically address the issue of non-linearities in gradients, of time-varying boundary motion, or of the non-planarity of discontinuities [50, 53].

Example Figure 11 illustrates an example of possible EIDOSCOPE observations during the crossing of a current sheet near the reconnection region. For Configuration 1, Fig. 11a, observations with three-scale variations along the current sheet are realized. EIDO can be used to determine the fluid/ion scale context, such as the orientation of the sheet and the plasma and field conditions on either side of reconnection X-line. This requires certain assumptions concerning the time-stationarity of the current sheet, its curvature, or its speed, which can all be obtained from one or more of the methods in

Table 3 Overview of some common methods and required measurements to infer some of the key parameters of plasma structures

		Orient	Veloc	Accel	Required data
Timing/triangulation methods[a]					
CVA	Constant velocity approach	X	X		Any quantity
CTA	Constant thickness approach	X	X	X	..
PVA	Polynomial velocity approach	X	X	X	..
DA	Discontinuity analyzer	X	X	X[b]	**B**
Gradient methods					
GRA	Gradient of any quantity	X			Any quantity
MVAcE	Minimum variance of $\nabla \times \mathbf{E}$	X	X		Full 3D **E** field
MDD[d]	Minimum directional derivative	X			**B**
STD[e]	Spatio temporal derivative		X	X	**B**
Single spacecraft & residue methods					
MVAB	Minimum variance of **B**	X			**B**
MVAE	Maximum variance of **E**	X			full 3D **E** field
HT	deHoffmann-Teller analysis		X	X	**E** (or **V** & **B**)
MFR	Minimum Faraday residue	X	X		**E** (or **V** & **B**)
MMR	Minimum massflow residue	X	X		**V**, **B** & n
COM[f]	Combination of above	X	X		

Additional information such as crossing duration can often be utilized to infer the thickness of a structure. For an overview of methods, see e.g., [50]. EIDOSCOPE will be able to utilize all these methods, sometimes on several scale sizes simultaneously. EIDOSCOPE will also provide a better assessment of error margins and the validity of assumptions

[a]In its simplest form, timing methods require minimum 2 spacecraft. Typically 4 spacecraft are used

[b]Additional information about orientation from e.g., single spacecraft methods needed

[c]Knowledge about the ∇ operator can also be used to estimate e.g., magnetic curvature

[d]The MDD method [51] can provide information about the dimensionality of a structure and orientation of 1D (e.g., boundary normal of current sheet) or 2D (e.g., axis orientation of a flux rope) structures

[e]The STD method [52] can provide velocity as function of time for a plasma structure

[f]Combining variance matrices from several spacecraft or several methods used to utilize all available information

Table 4 Magnetospheric multi-spacecraft mission ability to address physics at different scales

Mission	#	e^- scales	Ion scales	Fluid scales
Cluster small separation	4	1 point	**Tetrahed**	1 point
Cluster large separation	4	1 point	1 point	**Tetrahed**
Cluster multi-scale	4	1 point	**1 pair**	**3 point**
THEMIS	5	1 point	1 point	**multipoint**
MMS	4	**Tetrahed**	1 point	1 point
Cross-Scale	12	**Tetrahed**	**Tetrahed**	**Tetrahed**
SCOPE	5	**1 pair**	**Tetrahed**	1 point
EIDOSCOPE Config 1	6	**1 pair**	**Tetrahed**	**1 pair**
EIDOSCOPE Config 2	6	**2 pairs**	**Tetrahed**	1 point

1 point: single point measurements obtained while scanning through a structure can partially reveal features at the structure scale if it is time-stationary during the crossing. *Pair*: a pair of spacecraft can resolve spatial scales in one direction; two pairs allow in addition to identify the differences from one pair to another. *Tetrahedron*: 4 spacecraft allow the 3D exploration of spatial structure at the tetrahedron scale. *Multi-point*: irregularly spaced spacecraft sample the scale in an exploratory way

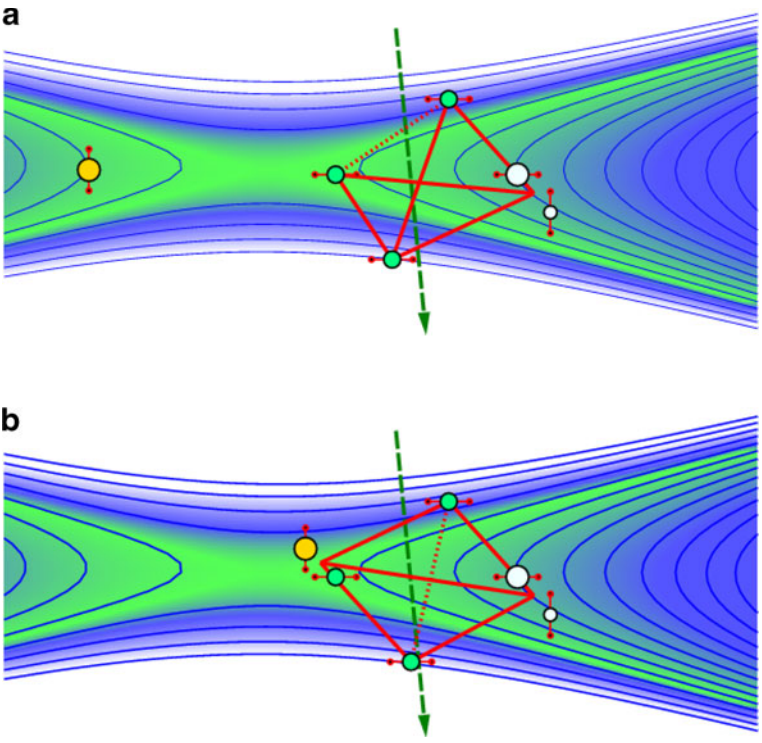

Fig. 11 Example of boundary layer determination using EIDOSCOPE. **a** EIDOSCOPE in Configuration 1. **b** EIDOSCOPE in Configuration 2. See text for details

Table 3. At the same time, the simultaneous ion/electron scale observations by the SCOPE spacecraft will resolve the overall thickness of the current sheet and the changes in the particle distribution functions across the sheet. This EIDOSCOPE configuration is also useful for checking the time-variability of moving structures along the current sheet. For Configuration 2 shown in Fig. 11b the pairs of spacecraft in the EIDOSCOPE configuration with electron scale separation resolve electron scale structure in the direction across the sheet (a 2 point problem at electron scales but with given orientation), as well as this structure along the sheet over ion scales (a 2 point problem at ion scales also with given orientation).

4 EIDOSCOPE mission

Spacecraft EIDO is a single spacecraft contribution to the SCOPE mission forming the common mission, EIDOSCOPE. SCOPE consists of 5 spacecraft—Mother, Near Daughter (ND) and 3 Far Daughter (FD) satellites (Fig. 12). The Mother and ND are currently developed and will be built by JAXA while

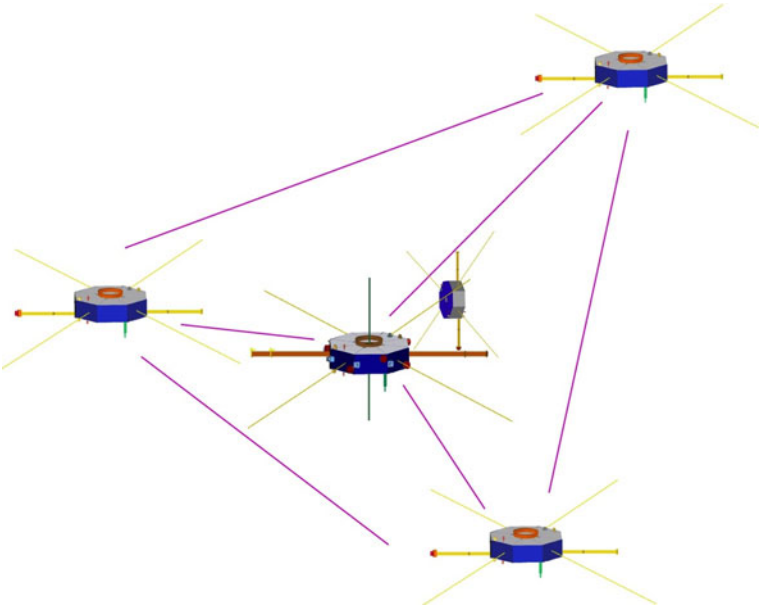

Fig. 12 SCOPE satellites

the 3 FD spacecraft will be built by the Canadian Space Agency (CSA). The EIDOSCOPE mission lifetime is 3 years with a possible extension of 2 years. The EIDO lifetime is limited due to the significant amount of fuel needed to keep the spin axis oriented toward the sun, presently sized for a full 5 year mission. The lifetime of the sun-pointing SCOPE Near Daughter is similarly limited to 2–3 years and thus in the extension phase EIDO would be the only spacecraft in the EIDOSCOPE constellation with a sun-pointing spin axis.

Launch All 5 SCOPE spacecraft will be launched on an H2-A rocket either directly into a highly elliptical high-apogee orbit or via geosynchronous transfer orbit. EIDO can be launched together with SCOPE with the same launcher H2-A by using about 49% of the H2-A spare launch mass capacity. From the injection orbit given by H2-A EIDO will take itself to the final orbit. The propulsion system for putting EIDO in the final orbit is assumed to use bi-propellant. The same propellant is used for spinning up, changing the constellation and attitude control. EIDO is designed in a way that, if required, it could also be launched by a separate launcher such as Vega. In this case an additional solid rocket motor would be needed to put EIDO into a similar orbit.

Orbit EIDOSCOPE will fly in an equatorial orbit with perigee 8–10 R_E and apogee 25–30 R_E. The inclination of the orbit is adjusted depending on the launch date so that the spacecraft apogee is in the center of the tailbox, the

scientific target of interest in the tail. The orbit inclination can therefore be within $\pm 14°$. Figure 13a illustrates the orbit for the case when the apogee crosses the tailbox during summer. Then, half a year later, Fig. 13b, the perigee of the orbit is at the inner edge of the tailbox and apogee is out in the solar wind. The amount of cumulative time spent in the tailbox is about 40 days per year.

Spacecraft configuration During the initial phase of the mission, ~1 years, the SCOPE spacecraft are kept close together (less than 100 km) while EIDO would approach from large distance down to ~1000 km distance, see Fig. 4. During the second phase the SCOPE spacecraft separation will be gradually increased up to ~5,000 km while at the same time EIDO will be close to one of the Far Daughter satellites, see Fig. 5. During the same phase and eventually also during the extension of the mission, the configuration where EIDO is somewhere in the center of SCOPE constellation will be realised, see Fig. 6.

Operational mode The satellite payload is continuously operating throughout the orbit. The exception is that the payload is switched off during the attitude and configuration maneuvers. Two data streams are constructed – *Summary Data* with lower data rate and *Burst Data* with full data rate. All Summary Data are stored on-board continuously and all of them are transmitted to the ground. Summary Data include particle moments, reduced distribution

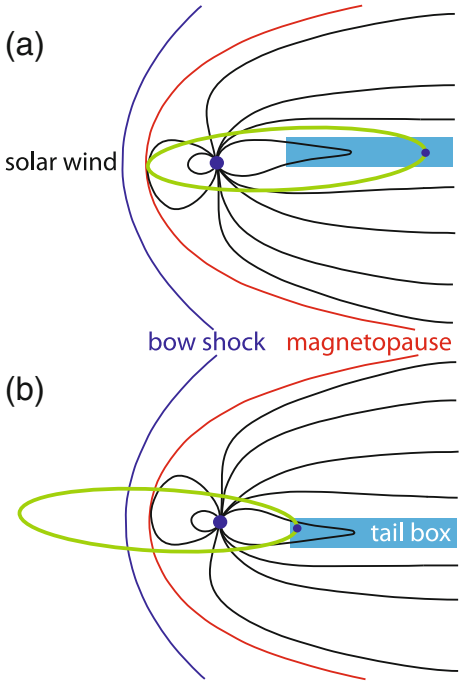

Fig. 13 EIDOSCOPE orbits with half a year separation. The tailbox is defined as a 4 R_E thick, 20 R_E long and 10 R_E wide box located around the most probable location of the tail current sheet

functions, sub-sampled wave fields and spectral information. Summary Data have high enough quality (sampling frequencies, resolution, phase space coverage, integrated particle moments) to satisfy large parts of the science goals of the mission. Summary Data are also used for the real-time selection of scientifically interesting intervals from which Burst Data should be transmitted to the ground. The time intervals that are identified for the download of Burst Data will be common for all EIDOSCOPE satellites. Burst Data are saved on-board continuously from most of the orbit but due to telemetry constraints only selected intervals can be transmitted to the ground. Burst Data with the oldest and lowest priority that have not been transmitted to the ground are continuously deleted to make room for the new observations. Approximately 2 orbits, 8–10 days, of Burst Data can be kept on-board.

Communication The SCOPE Mother will use X-band for both up- and downlink, with the intersatellite communications and ranging system operating in S-band. The Near Daughter communicates through the Mother, including data downloads. The Far Daughters communicate to ground in S-band or through Mother, but data are always downloaded directly to ground. EIDO will use S-band for both up and downlink, with the capability to participate in the SCOPE intersatellite communications and ranging system operating in S-band. The SCOPE ground communication is based around a 64 m dish at the Usuda Deep Space Center and a 34 m dish at the Uchinoura Space Center (both in Japan). The EIDO ground communications can make use of ESA 15 m or 35 m antennae supporting S-band. The possibility of using ESA antennae for increased data return from SCOPE satellites should be considered.

Ground segment The SCOPE ground segment consists of three operational entities: Science Operations Center (SOC), JAXA Mission Operations Center (MOC) and CSA MOC. The EIDO ground segment consists of an ESA MOC. In addition, ESA would participate in the SOC that would be run jointly by JAXA, CSA and ESA. The SOC is responsible for the science planning, data retrieval, data processing and data archiving of the science data from the whole EIDOSCOPE mission. The JAXA MOC is responsible for the operations of the Mother and ND and also for the uplink of the FD spacecraft commands generated by the CSA MOC when inter-spacecraft separation is less than 100 km. The CSA MOC is responsible for the operations of the FD spacecraft. The ESA MOC is responsible for the operation of the EIDO spacecraft. In practice, the MOC's and the SOC will work closely together, benefiting from common activities and interests. Shared ground-station activities are likely to optimise the data return for the mission.

International collaboration There is large international interest in the EIDOSCOPE mission. Potential participation could include provision of flight hardware, collaboration in the mission design, and the contribution of additional daughter spacecraft. Additional spacecraft could be used to improve resolution and coverage of fluid or electron scales, or even larger system-scale monitor-

ing. Possible partners include major space agencies such as NASA as well as smaller national space agencies or individual laboratories.

Synergies with ground-based and low altitude observations Very strong synergy can be expected by combining EIDOSCOPE observations with ground-based observations, including: global ground based observations of large areas of the ionosphere (such as the SuperDARN project comprising radars with global coverage of the polar regions); high resolution multi-point localized measurements (such as auroral cameras, ground-based magnetometers and high resolution incoherent radar observations); low-orbit in-situ observations in conjunction with EIDOSCOPE. Such EIDOSCOPE-ground based observation synergies can be particularly efficient in studying regions of particle acceleration in current sheets and jet fronts in the magnetotail. The structures resolved by EIDOSCOPE in the magnetotail map to ionospheric structures of a few km to a few hundred km in size, which is well resolved with ground-based instrumentation. Furthermore, the magnetic footprint of EIDOSCOPE near perigee moves very slowly in geographic coordinates, allowing extended comparisons. Figure 14 shows the magnetic footprint moving across the fields of view of ground-based all-sky cameras over a period of 13 hours.

Ground-based networks Large scale imaging of the ionosphere also adds continuous monitoring of magnetospheric physical processes on the system scale that are not covered by EIDOSCOPE. There are relatively dense ground-based networks both in Canada and Northern Scandinavia. The Canadian GeoSpace Monitoring network offers the capability for excellent detailed conjunction studies, which have been established during the preparation of the SCOPE

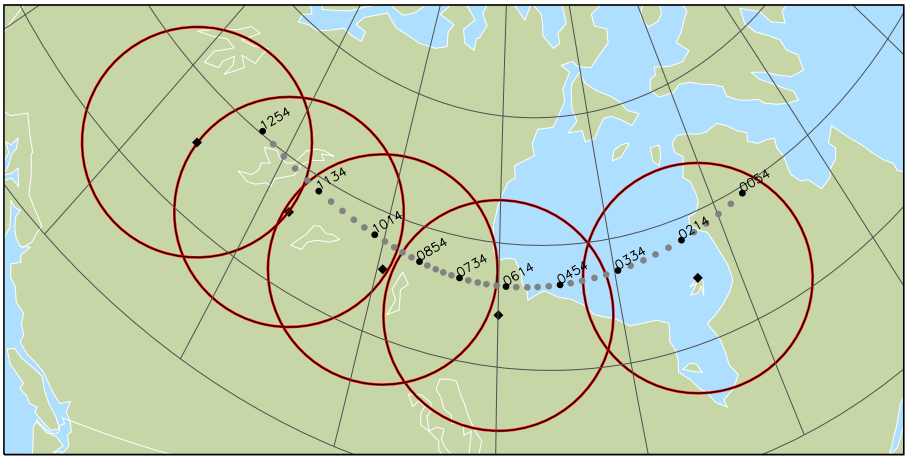

Fig. 14 EIDOSCOPE magnetic footpoints superposed on a map showing fields of view of all-sky cameras. The *dots* are separated by 16 min, with every 5th point highlighted and its corresponding UT shown (courtesy Eric Donovan)

project. Furthermore, recently-developed phased-array radars at Poker Flat and Resolute Bay allow comprehensive 3D monitoring of the ionosphere at many times higher temporal and spatial resolution than before. A similar system, EISCAT 3D, is planned to be deployed in the future in Northern Fenno-Scandinavia. All of these radars will be running for many years before the launch of EIDOSCOPE and thus will have accumulated sufficient expertise in operations to become an efficient tool for conjunction studies.

Synergies with numerical simulations Numerical simulation support is indispensable in the analysis of the data, and also forms an important element during the planning stages to maximize the science return from the mission. The EIDOSCOPE team has close links to many numerical simulation teams who will provide the required support. Of particular importance will be results from a range of different types of numerical simulations (MHD fluid, hybrid, full-particle) to optimize the cross-scale aspects of the mission. The planning for EIDOSCOPE will likewise serve to focus numerical simulation studies toward the issues of multi-scale physics. This focused effort will bring new simulation methods (e.g., seamless merger between a fluid code and a particle code), new research schemes (e.g., mechanisms and support to share results from a huge simulation run that is feasible in a limited number of facilities) and potential breakthroughs in Plasma Universe research across the disciplines that EIDOSCOPE will foster during the mission.

5 EIDO design

Spacecraft Figure 15 shows a possible design of the EIDO spacecraft. The spacecraft has an octagonal shape, of overall diameter 2 m and height 1.5 m. EIDO is a spin-stabilized satellite with spin axis pointing towards the Sun. The spin axis angle is kept $<10^\circ$ with respect to the Sun. The propellant consumption for attitude control is determined mainly by the requirement to keep the spin axis pointing at the sun. Instruments are located on the upper deck below the solar panels. Four fuel tanks are symmetrically located. A possible layout of the instruments is shown in Fig. 16.

EIDOSCOPE payload overview Table 5 provides an overview of the baseline instrument payload on all EIDOSCOPE spacecraft. Due to the specifics of the EIDOSCOPE mission, the payload differs among the spacecraft. High accuracy measurements covering fields and particles require large spacecraft such as the SCOPE Mother and EIDO while many multi-point measurements are obtained using the more modestly equipped SCOPE Far Daughter satellites. The SCOPE Mother employs newly-designed particle instruments: (1) FESA to obtain 10 msec electron sampling in the low density region of the magnetotail, and (2) MESA/MIMS to cover the energy range up to 100–200 keV, with significantly better resolution and geometric factor than has been possible until now. The least equipped SCOPE Near Daughter has a sun-pointing spin

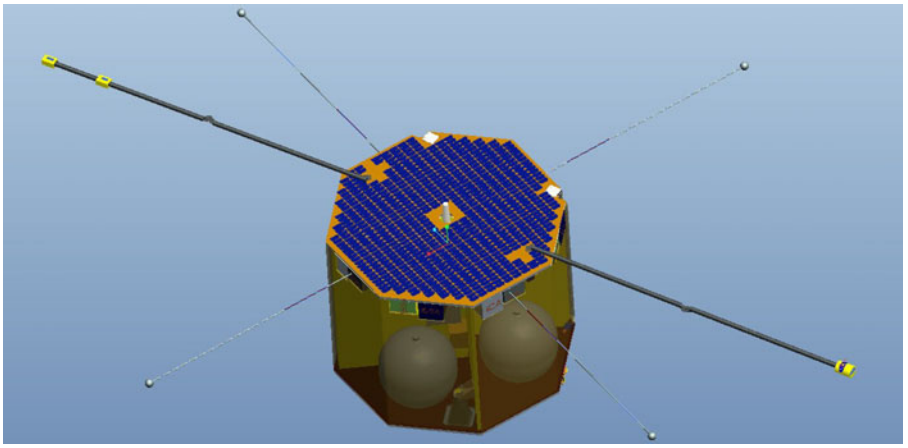

Fig. 15 Possible overall design of spacecraft

axis with 60 m tip-to-tip wire booms and complements the SCOPE Mother spacecraft in order to measure the full 3D electric fields at relatively low frequencies. At higher frequencies, the Mother/Near Daughter pair resolves 2D electric fields at two points separated by electron scales. All SCOPE spacecraft in addition have axial booms to measure, with less precision, the local 3D electric fields (AC). The baseline payload of EIDO consists almost entirely of proven technology, with heritage from recent missions (e.g., Cluster, Polar, THEMIS, STEREO) combined with newly-developed concepts already selected in the context of future missions (e.g., Bepi-Colombo, Solar Orbiter, MMS).

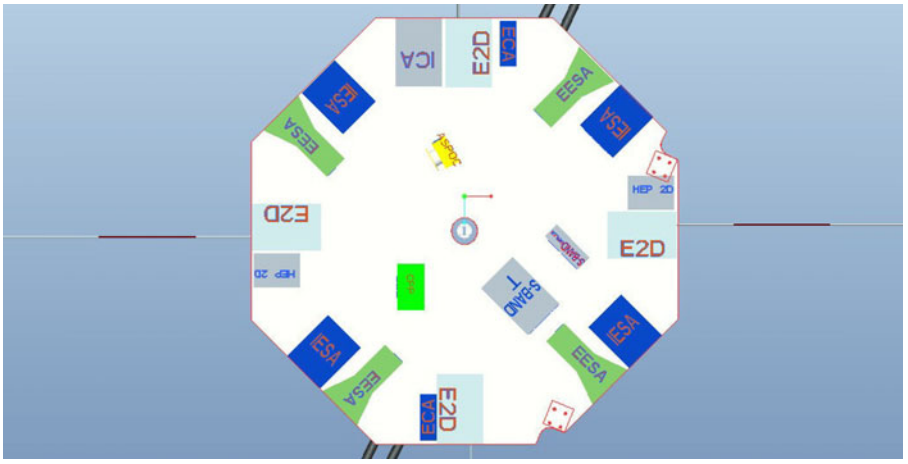

Fig. 16 Possible layout of instruments on the spacecraft

Table 5 SCOPE and EIDO science instrumentation

Quantity	Mother	Near Daughter	Far Daughters	EIDO
Electrons	FESA 10 eV–30 keV 32 × 8 × 16 @ 125 S/s	–	EISA 0.01–20 keV/q 32 × 8 × 16 @ 1/4 spin	EESA 3 eV–30 keV 32 × 8 × 16 @ 50 S/s
	MESA 10–60 keV 16,32 × 8 × 16 @ 1/2 spin			–
	HEPE 30–700 keV 8 × 8 × 16 @ 1 spin			HEP 20–800 keV 10 × 8 × 16 @ 1/2 spin
Ions	FISA 5 eV/q–30 keV/q 32 × 8 × 16 @ 1/8 spin	–		IESA 3 eV–40 keV 32 × 8 × 16 @ 1/4 spin
	IMSA 20 eV/q–20 keV/q, 8 spec. 32 × 8 × 16 @ 1/2 spin			ICA 10 eV–40 keV, 4 spec 32 × 8 × 16 @ 1/2 spin
	MIMS 10–180 keV/q, 5 spec. 16,32 × 8 × 16 @ 1/2 spin			ECA 5keV–1MeV 8 × 6 × 12 @ 1/2 spin
	HEPI 160–2,000 keV 12 × 8 × 16 @ 1 spin			HEP 40keV–1MeV 10 × 9 × 18 @ 1/2 spin
Particles & fields	O-WPIA correlator @ 20 kS/s	–	–	–
Magnetic field	MGF 128 S/s	MGF 128 S/s	MG 128 S/s	MAG 128 S/s
	OFA/WFC-B 20 kS/s	OFA/WFC-B 20 kS/s	OFA/WFC-B 20 kS/s	ACB 30 kS/s
Electric field	EFD 64 S/s	EFD 64 S/s	EFD 64 S/s	E2D 300 kS/s
	OFA/WFC-E 100 kS/s	WFC-E 100 kS/s	WFC-E 100 kS/s	
	HFR 10 kHz–10 MHz	HFR 10 kHz–10 MHz	HFR 10 kHz–10 MHz	–

Particle instrument resolutions are given as the number of energy × polar × azimuthal bins @ best 3D time resolution. The nominal spin period is 3 s for Mother, Near Daughter and Far Daughters and 4 s for EIDO

Science requirements on EIDO payload The science requirements on the EIDO payload are summarized in Table 2. The requirements **R1,R5-R8** deal with instrument temporal resolution as compared to typical scales in plasma. Figure 17 shows the typical characteristic spatial and temporal scales within the plasmas that we expect EIDOSCOPE to encounter. The spatial scales can be converted to temporal scales by applying a Doppler shift corresponding to the characteristic plasma boundary speeds, i.e., 100-1000 km/s (black and red dotted lines in Fig. 17). Figure 17 also summarizes all the EIDO baseline instruments, their temporal resolution and how the resolution compares to the characteristic electron/ion/fluid scales, as required by the science requirements **R1,R5-R8**. The requirements **R5-R8** deal with plasma particle measurements, typical expected plasma parameters are shown in Fig. 2.

EIDO payload The EIDO baseline payload will consist of a full set of plasma instruments, including AC and DC magnetometers, four wire probe antennas to measure AC and DC electric fields in the spin plane, as well as thermal ion, electron and ion composition instruments for measurements of the 3D particle

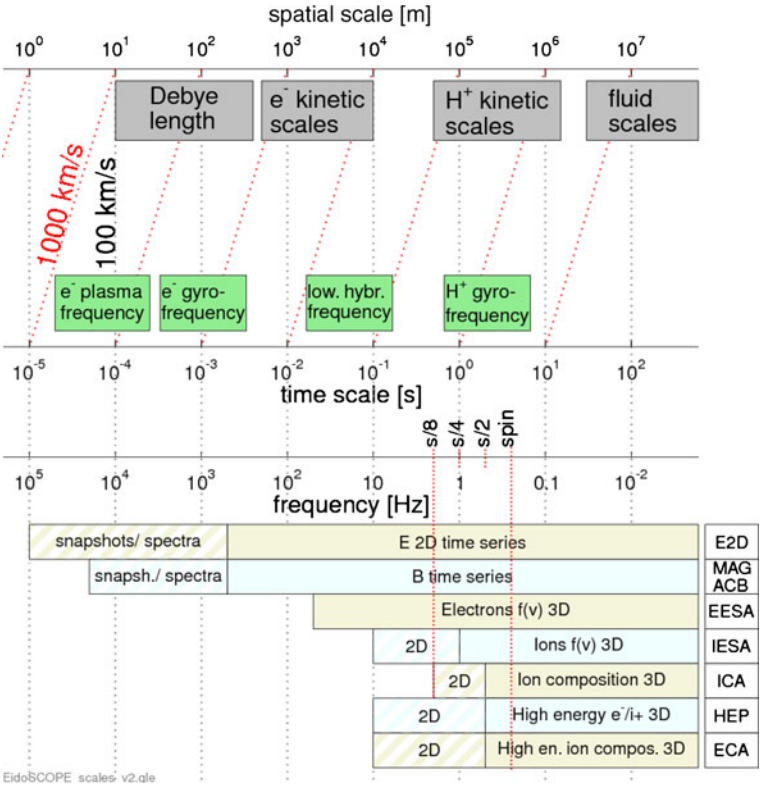

Fig. 17 Typical temporal and Doppler shifted spatial scales of physical processes and their comparison to the temporal resolution of EIDO instrumentation

Table 6 Description of EIDO payload

Instrument	Short description
MAG DC magnetometer	Dual-sensor instrument based on flux gate technology, measuring ambient magnetic field. Heritage: Cluster, Double Star, THEMIS etc.
ACB AC magnetomteter	Tri-axial search coil instrument composed of 3 ELF/VLF antennae. Heritage: Cluster, DEMETER, THEMIS, MMS etc.
E2D wire boom electric field	Four wire probe antennae extending 40–50 m from the spacecraft. Electronics hardware includes an active electron density sounder. Heritage: Cluster, THEMIS, MMS, Bepi-Colombo etc.
EESA electron spectrometer	Four dual top-hat electrostatic analysers arranged around the spacecraft to obtain the full 3D distribution function of electrons at high time resolution. Adaptive geometric factors. Heritage: Freja, STEREO, MMS, Bepi-Colombo etc.
HEP energetic electron/ion spectrometer	Instrument based on solid state detector technology with a pin-hole entrance aperture. Baseline: two detector sets placed on opposite sides of the spacecraft. There is option of using newly-developed design that among other things provides a larger instantaneous field-of view. Heritage: Cluster, MMS etc.
IESA ion spectrometer	Four top-hat analysers arranged around the spacecraft to obtain the full 3D distribution function of ions at high time resolution.
ICA ion composition spectrometer	360° top-hat electrostatic analyser capable of obtaining and discriminating the full 3D distribution function of major ion species (H^+, He^+, He^{++}, O^+).
ECA energetic ion composition spectrometer	Time-of-flight vs. pulse-height sensor to obtain composition measurements of energetic ions. It will resolve as a minimum H^+ and O^+ ions but there is a capability to resolve also He ions. Heritage: Geotail, IMAGE, MMS etc.
CPP central payload processor	This processor will serve all the particle and field instruments. A common processor for the whole instrument suite eases the stringent time synchronization requirements, simplifies coordinated data sampling and simplifies the interface presented to the spacecraft.
Optional instrumentation	Faraday Cup for solar wind measurements with very high time resolution. Potential control device ASPOC allowing to improve low energy ion and electron measurements.

distribution functions and their moments (density, mass flux, etc.). Because the core theme of EIDO is particle acceleration, EIDO will provide high time resolution measurements of energetic particles including ion composition. Table 6 gives the short summary of each instrument and Table 7 specifies the Technology Readiness Levels (TRL), mass, power and data rate budget for each instrument.

Data rates Table 8 gives the data rates generated by the whole EIDOSCOPE mission and each spacecraft separately. The data rates depend on the way

Table 7 EIDO TRL, mass, power and data rate budget

Instrument	TRL	DMM	Mass (kg)	Power (W)	Summary data (kbytes/s)	Burst data (kbytes/s)	Compres.
MAG	9	10%	1.03	1.65	0.37	–	2
ACB	8	10%	0.88	0.11	0.91	93.7	2
E2D	8	10%	8.80	0.44	1.41	125.5	2
EESA	6	20%	14.40	33.60	6.18	118.1	8
HEP	9 (2)	20%	2.40 (4.08)	3.12 (4.8)	0.24 (1.25)	1.5 (7.5)	8
IESA	6	20%	7.20	9.60	0.60	2.60	8
ICA	8	10%	3.85	6.60	1.21	4.2	8
ECA	5	20%	2.20	2.20	0.45	3.0	8
CPP	5	20%	6.00	19.20	–	–	–
Total			46.76	76.52	11.36	348.6	

The mass of the magnetometer booms are excluded. Mass and power are given including Design Maturity Margin (DMM). Compressed data rates for Summary and Burst data are specified. Compression column shows the used compression factor for the Burst Data. HEP optional parameters are in brackets

Burst Data and Summary Data are formed and will require coordination among the EIDOSCOPE partners; these will be adjusted and refined during the Assesment phase.

Sun-pointing EIDO The baseline proposition is to have EIDO as a sun-pointing spin axis spacecraft, with spin period 4 s and spin axis $<\sim 10^\circ$ from the Sun. There are several very important advantages in this choice driven by EIDO's science objectives and associated requirements. The sun-pointing EIDO spacecraft allows high precision electric field measurements to be made. Wire booms can be made much longer than axial booms, yielding significantly lower noise levels and higher absolute accuracy. Moreover, even with wire booms, the most sensitive and accurate measurements are in the direction perpendicular to the solar direction, since booms oriented along the solar

Table 8 Approximate compressed data rates, data volumes, storage; downlink speed and required downlink times

	Mother	ND	Single FD	EIDO	Total
Stored data rate					
Burst data (kbyte/s)	350–630	4–290[b]	14–300	350	6–2,770
Burst data (Gbyte/day)[a]	29–52	0.33–24	1.2–25	29	61–179
Summary data (kbyte/s)	16–42	1.55	4.4–12	11.4	91
Summary data (Gbyte/day)	1.3–3.5	0.13	0.4–1.0	0.94	3.5–7.5
Storage capacity	50–100 GB	–	9–20 GB	100 GB	
Downlink speed	4 Mbps	–	400 kbps	600 kbps	
Required downlink time					
10 min burst data	0.12–0.31 h	–	0.05–1 h	0.78 h	1.03–3.99 h
Daily summary data	0.84–2.09 h	–	2.1–5.8 h	3.65 h	23 h

[a] Assumes 100% of the burst data are saved

[b] Data saved on Mother

direction are more prone to errors from wake and asymmetric photoelectron cloud effects. This can be seen in Fig. 18, which illustrates the use of different antennae and wire boom directions on THEMIS. By having two components perpendicular to the sun, EIDO will be able to meet the sensitivity requirements **R2,R3** in Table 2. The sun-pointing characteristic of EIDO offers also a unique capability to inter-calibrate instruments between EIDO and the nearby Far Daughter satellite. This is particularly useful for the magnetic field instruments (MAG, ACB), where the spin axis component is significantly more difficult to calibrate. These instruments can be cross-calibrated against the partner spacecraft's spin-plane measurements. It will also be useful for inter-calibration of E2D and the particle instruments.

3D electric field By locating EIDO close to one of the SCOPE Far Daughters, EIDO will form another pair similar to the SCOPE Mother/Near Daughter. This configuration will be excellent for 3D electric field measurements by having wire boom measurements in all 3 directions, satisfying the requirement **R4**. Electric field data from the instruments on the close pair can be used to inter-calibrate each other's measurements and minimise errors associated with wake effects, spurious electric fields resulting from spacecraft charging and offsets due to asymmetric photoemission. For scale sizes larger than the EIDO - FD separation, the EIDO and FD electric field measurements can be combined to give the full 3D electric field including any non-zero parallel (E·B) electric field. At smaller scale sizes (typically near the electron scale), the paired satellites provide two-point measurements with wire-boom measurements in 2 orthogonal planes.

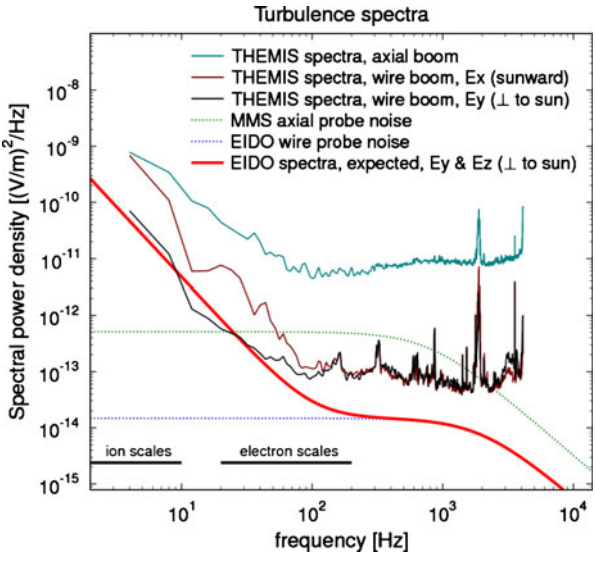

Fig. 18 Comparison of electric field spectra in the solar wind from different THEMIS probe measurements. Sun-pointing EIDO will measure two high quality components of electric field perpendicular to the Sun-Earth line that are crucial to get physics right at electron/ion coupling scales

Attitude EIDO is a spin-stabilized satellite with spin axis pointing towards the Sun. The spin axis angle is kept $<10^\circ$ with respect to the Sun. The propellant consumption for attitude control is determined mainly by the requirement to keep the spin axis pointing at the sun. For attitude determination EIDO will employ a star tracker. To keep the EIDO spin axis within 10° from the Sun, EIDO will require attitude adjustments at least once every 10 days. Attitude adjustments are done by a pair of thrusters mounted on the sides of the spacecraft body. They use the same bi-propellant system as the main spacecraft propulsion. The propellant consumption for precessing the spin axis, for spinning up the spacecraft and for deploying the booms is ∼67 kg for five years. It is mainly driven by the moment of inertia residing in the E2D instrument wire booms. During attitude maneuvers high voltage instruments will be required to be switched off for several hours.

Formation flying EIDO will have to fly in a formation with the SCOPE satellites. SCOPE uses inter-satellite ranging technology to determine the relative distances between satellites to ∼10 m. The traditional orbit-determining precision from the ground for ranging orbits of this kind is ∼10 km with possible later orbit reconstruction to ∼100 m. The SCOPE satellites will approach each other as close 1 km, basing their navigation on the inter-satellite ranging. EIDO will use the same inter-satellite ranging technology and will be able to estimate its location within the SCOPE constellation with high precision when in the range of inter-satellite ranging. However, EIDO will not approach closer than 10 km to the Far Daughter satellite during the nominal mission. For safety EIDO will stay on an orbit with different orbital elements. The EIDO orbit during the nominal mission should be far enough from the nearest satellite to allow ground ranging and control of the EIDO orbit within the necessary safety margins.

Satellite reconfiguration Controlling the satellite configuration requires propellant both when changing the satellite separation to a new configuration as well as maintaining the configuration at some given separation scale. The fuel costs of keeping satellites at a defined separation scale (orbit maneuvers once every few orbits) varies approximately linearly with the spacecraft distance; orbit corrections are necessary about once every 10 orbits. Table 9 summarizes the expected requirements on the fuel or ΔV. For example, 1000 km reconfiguration costs ∼10 m/s in ΔV and the maintenance of such configuration ∼8 m/s yearly. The total mission ΔV is estimated to 300 m/s including 100% contingency.

Telemetry Since the EIDO spin axis is sun-pointing, the angle between the spin axis and the Earth ground station will vary throughout the orbit. To have continuous contact with the Earth ground stations, two communication antennas are mounted on the spin axis, one on each side of the satellite, covering both hemispheres. The spacecraft switches between the two antennae depending on the Earth's location.

Table 9 Fuel/ΔV requirements during the satellite deployment and reconfiguration assuming 50 m wire boom length

Operation	Distance	ΔV or fuel [kg]
Wire-boom deploym.	–	∼7 kg fuel
Maintain formation	L km	∼0.008 m/s/L/year
Formation change	L km	∼0.01 m/s/L
Spin axis orientation	–	∼12 kg/year

Clock synchronization To satisfy science requirement **R9** the relative precision on data sampling among satellites shall be within L/1000 ms where L is the satellite separation in km. For 100 km separation this implies 100 μs precision. Using ground reconstruction, the reconstructed EIDO clock drift is less than 1 ms after 3 days of non-contact with ground. This precision will satisfy the science requirement **R9** for separations of ≥1000 km. For smaller separations EIDO will have to use SCOPE ranging system to synchronize clocks. EIDO separation will be at all times >10 km and therefore the highest requirement on clock precision is 10 μs. Clock synchronization can then be achieved either taking an active part in the inter-satellite communication or by listening to the SCOPE Mother to Daughter satellite transmissions and locking the EIDO clock to the Mother clock.

Mass budget EIDO mass budget is given in Table 10. The total mass of 697 kg is compatible with the capability of H2-A to carry, in addition to SCOPE, additional load with total mass ≥1430 kg.

Table 10 EIDO mass budget

Subsystem	CBE	DMM	CBE + DMM
Power	43.61	10%	47.97
TM & communic.	11.10	6%	11.70
Data handling	6.20	5%	6.60
Structure & mechan.	65.39	20%	73.15
Thermal control	5.90	20%	7.11
Harness	7.00	20%	8.40
Stiff booms	3.00	20%	3.60
Propulsion system (excl. propellant)	48.00	20%	57.60
ISL transponder (excl. antennas)	5.0	20%	6.00
Payload	40.24	16%	46.76
Balancing mass	5.00	0%	5.00
Total s/c dry mass w/o margin			273.89
System level margin 20%			54.78
Total s/c dry mass			328.67
Propellant spin-up & precession			67.00
Propellant final orbit & mission Δv			201.15
Total spacecraft mass			596.82
Launcher adapter			100
Total mass installed on H2-A			696.82

Table 11 EIDO power budget in W

Subsystem	Sun	Eclipse
Avionics	22.2	22.2
RF system	68.0	8.0
AOCS	4.3	4.3
Propulsion	5.5	5.5
Thermal	0	20
Power S/S	16.8	16.8
Total platform	116.8	76.8
Payload	76.5	76.5
Total	193.2	153.3
Total (incl. 20% margin)	231.9	183.9

Power budget Table 11 shows the total power budget of EIDO. The solar arrays cover $\approx 2\,m^2$ of the sun-oriented surface. This gives a maximum available power of 740 W. Taking into account degradation of solar cells and possible loss of solar cell strings, we estimate that this will provide ≈400 W, at end-of-life. The transfer stage to the final orbit may impose a requirement to have solar panels on the side of the spacecraft body as well because the spin axis of the spacecraft may not point straight at the sun; this is taken into account in mass budget. The battery sizing is based on a worst-case eclipse load of 184 W and duration 6 h. In eclipse the transponder is assumed to be turned off (−60 W) and replaced by a heater dissipating +20 W.

Environmental constraints The electromagnetic cleanliness requirements are similar to earlier missions such as Cluster, MMS, and THEMIS. The radiation environment during the complete mission lifetime is expected to be less than 60 krad (1.5 mm) and 10 krad (4 mm), and hence does not appear to be problematic. EIDO will need to be compliant with all the management, design and operational requirements on space debris mitigation for ESA Projects.

6 Science Operations and Archiving

Management The EIDOSCOPE Science Operations Centre (SOC) will have responsibility for the science planning, data retrieval, and data processing. The SOC will be responsible for receiving inputs from the science working teams (SWT) together with detailed instrument commanding from the PI teams. The SOC will be responsible for coordination of these inputs to form a joint science operations plan that will be passed to the MOCs for implementation. Previous missions, notably Cluster and Double Star, have adopted such a joint strategy. The relatively close formation of EIDO and SCOPE together with the science objectives that require detailed comparison and manipulation of data across the various spacecraft will require an effective and efficient joint operations strategy and mechanism. Common data formats and data access will ensure that the science objectives can be met through analysis of data from all the spacecraft involved. The reduction from raw data to science-quality data products will be the responsibility of the individual PIs.

Community input The PI teams, SWT, and SOCs form the natural routes for community input into the science and mission planning. Ground-based observations will extend the science objectives both by providing a global scale, e.g., as imaged in the auroral regions, and by employing EIDOSCOPE data for studies of the Sun/Earth connection. In the first instance, this would be done through representation at SWT level but it could involve coordination between, for example, EIDOSCOPE and ground-based SOCs.

The onboard Data Handling System (DHS) DHS will store, prioritise, pack, and transmit science and housekeeping data. The science instruments generate raw data at a rate of roughly 340 kBytes/s (after compression) or 160 GBytes over 2 full orbits. The DHS will need to store this data to enable it to be telemetred, in whole or selected subintervals, via contact periods with the mission ground stations. Depending on the available telemetry, selection will be made on the basis of visual inspection of quick-look data or pre-determined time intervals based on orbit predictions. Onboard triggering of science events will be implemented for SCOPE. It may be envisaged for EIDO as well, but would in any case be impractical across the EIDOSCOPE constellation without inter-satellite communication. The SOC will need to ensure that the telemetred intervals of highest resolution data for EIDO and SCOPE match.

Data production The Summary Data will be hosted by the ESDS for public access. In addition to its role in the SOC's selection of full-resolution data for download, the Summary Data will aid the SOC in future science planning. The Summary Data form the mission Quick-Look products and will be put online within 24 hours of ground receipt. Reduction of the full instrument data to high-quality science products will be the responsibility of the PI institutes in conjunction with facilities run by their National Agencies. This will involve a two-stage process. Within one month of receipt, initial versions of the science data will be generated based on ground-calibration information updated using inflight experience and refinements. Calibrated full-resolution data will be delivered to the ESDS within 3 months of ground receipt and will be open to the public.

Data access EIDOSCOPE will establish an EIDOSCOPE Science Data System (ESDS) during the early phases of the mission, e.g., by the selection of an ESDS PI. The ESDS will provide both EIDOSCOPE and the wider public a web-based interface to the mission data products. It is expected to conform to emerging Virtual Observatory standards, for example data being conformant with the SPASE standards. Good heritage and practice from the Cluster Science Data System [54] together with ongoing web-based data analysis tools such as Automated Multi Dataset Analysis [55] will ensure open access in an efficient and user-friendly environment. We would expect the long-term archive to be held by the Agency(ies), building on the CAA heritage. In this case, we would expect the ESDS and mission archive to be transparently connected rather than independent; this requires early planning.

7 Outlook

Recently a Forum on the Future of Magnetospheric Physics organized by the International Space Science Institute has identified particle acceleration and cross-scale coupling as the key outstanding topics to be addressed in future near-Earth space missions. This requires multi-spacecraft missions on multiple scales—an endeavor, which can only be implemented via interagency collaboration. We have described a multi-spacecraft mission concept EIDOSCOPE where by adding a single ESA spacecraft EIDO to JAXA/CSA mission SCOPE makes possible to address some of the key science questions of particle acceleration related to cross-scale coupling in space plasma, particularly at plasma boundaries. We show that having sun-pointing EIDO with comprehensive plasma payload gives decisive advantages in obtaining high quality data necessary to address those questions. The next years are crucial to finalize the definition of the next multi-spacecraft multi-scale mission that will serve the science community after current and upcoming multi-spacecraft missions Cluster, Themis and MMS. EIDOSCOPE offers ESA excellent opportunity for a fraction of M-class mission costs to become and integral part of major multi-agency mission addressing outstanding science questions.

Acknowledgements We acknowledge the support by the Swedish National Space Board that particularly allowed the Swedish Space Corporation to carry out feasibility study. We acknowledge the useful discussion and comments from A. Alexandrova (IWF, Austria), M. André (IRF, Sweden), G. Belmont (LPP, France), J. Birn (LANL, US), D. Burgess (QMUL, UK), J. P. Eastwood (ICL, UK), H. Hasegawa (ISAS/JAXA, Japan), S. Imada (ISAS/JAXA), A. Kis (GGKI, Hungary), L. Kistler (UNH, US), M. Oka (UCB, Berkeley), H. Opgenoorth (IRF, Sweden), G. Paschmann (MPE, Germany), V. Sergeev (Univ. StPB, Russia). We acknowledge the input from ISSI group "Dispersive cascade and dissipation in collisionless space plasma turbulence—observations and simulations".

References

1. Alfvén, H.: The plasma universe. Phys. Today **39**, 22–27 (1986). doi:10.1063/1.881039
2. Yamada, M., Kulsrud, R., Ji, H.: Magnetic reconnection. Rev. Mod. Phys. **82**, 603–664 (2010). doi:10.1103/RevModPhys.82.603
3. Martin, P., Apolloni, L., Puiatti, M., Adamek, J., Agostini, M., Alfier, A., Annibaldi, S., Antoni, V., Auriemma, F., Barana, O., Baruzzo, M., Bettini, P., Bolzonella, T., Bonfiglio, D., Bonomo, F., Brombin, M., Brotankova, J., Buffa, A., Buratti, P., Canton, A., Cappello, S., Carraro, L., Cavazzana, R., Cavinato, M., Chapman, B., Chitarin, G., Dal Bello, S., De Lorenzi, A., De Masi, G., Escande, D., Fassina, A., Ferro, A., Franz, P., Gaio, E., Gazza, E., Giudicotti, L., Gnesotto, F., Gobbin, M., Grando, L., Guazzotto, L., Guo, S., Igochine, V., Innocente, P., Liu, Y., Lorenzini, R., Luchetta, A., Manduchi, G., Marchiori, G., Marcuzzi, D., Marrelli, L., Martini, S., Martines, E., Mccollam, K., Menmuir, S., Milani, F., Moresco, M., Novello, L., Ortolani, S., Paccagnella, R., Pasqualotto, R., Peruzzo, S., Piovan, R., Piovesan, P., Piron, L., Pizzimenti, A., Pomaro, N., Predebon, I., Reusch, J., Rostagni, G., Rubinacci, G., Sarff, J., Sattin, F., Scarin, P., Serianni, G., Sonato, P., Spada, E., Soppelsa, A., Spagnolo, S., Spolaore, M., Spizzo, G., Taliercio, C., Terranova, D., Toigo, V., Valisa, M., Vianello, N., Villone, F., White, R., Yadikin, D., Zaccaria, P., Zamengo, A., Zanca, P., Zaniol, B., Zanotto, L., Zilli, E., Zohm, H., Zuin, M.: Overview of RFX-mod results. Nucl. Fusion **49**, 104019 (2009)

4. Cordey, J., Balet, B., Bartlett, D., Budny, R., Christiansen, J., Conway, G., Eriksson, L., Fishpool, G., Gowers, C., Haas, J.: Plasma confinement in JET H mode plasmas with H, D, DT and T isotopes. Nucl. Fusion **39**, 301 (1999)
5. Hellinger, P.: Structure and stationarity of quasi-perpendicular shocks: numerical simulations. Planet. Space Sci. **51**(11), 649–657 (2003). doi:10.1016/S0032-0633(03)00100-4
6. Zhong, J., Yutong, L., et al.: Modelling loop-top X-ray source and reconnection outflows in solar flares with intense lasers. Nat. Phys. **6**, 984–987 (2010). doi:10.1038/nphys1790
7. Baumjohann, W., Paschmann, G., Luehr, H.: Characteristics of high-speed ion flows in the plasma sheet. J. Geophys. Res. **95**, 3801–3809 (1990). doi:10.1029/JA095iA04p03801
8. Phan, T.D., Kistler, L.M., Klecker, B., Haerendel, G., Paschmann, G., Sonnerup, B.U.Ö., Baumjohann, W., Bavassano-Cattaneo, M.B., Carlson, C.W., DiLellis, A.M., Fornacon, K.H., Frank, L.A., Fujimoto, M., Georgescu, E., Kokubun, S., Moebius, E., Mukai, T., Øieroset, M., Paterson, W.R., Reme, H.: Extended magnetic reconnection at the Earth's magnetopause from detection of bi-directional jets. Nature **404**, 848–850 (2000)
9. Innes, D.E., Inhester, B., Axford, W.I., Wilhelm, K.: Bi-directional plasma jets produced by magnetic reconnection on the Sun. Nature **386**, 811–813 (1997). doi:10.1038/386811a0
10. Shibata, K., Nakamura, T., Matsumoto, T., Otsuji, K., Okamoto, T.J., Nishizuka, N., Kawate, T., Watanabe, H., Nagata, S., UeNo, S., Kitai, R., Nozawa, S., Tsuneta, S., Suematsu, Y., Ichimoto, K., Shimizu, T., Katsukawa, Y., Tarbell, T.D., Berger, T.E., Lites, B.W., Shine, R.A., Title, A.M.: Chromospheric anemone jets as evidence of ubiquitous reconnection. Science **318**, 1591 (2007). doi:10.1126/science.1146708
11. Ouyed, R., Pudritz, R.E., Stone, J.M.: Episodic jets from black holes and protostars. Nature **385**, 409–414 (1997). doi:10.1038/385409a0
12. Fermi-Lat Collaboration, Members of the 3C 279 Multi-Band Campaign, Abdo, A.A., Ackermann, M., Ajello, M., Axelsson, M., Baldini, L., Ballet, J., Barbiellini, G., Bastieri, D., et al.: A change in the optical polarization associated with a γ-ray flare in the blazar 3C279. Nature **463**, 919–923 (2010). doi:10.1038/nature08841
13. Masuda, S., Kosugi, T., Hara, H., Tsuneta, S., Ogawara, Y.: A loop-top hard X-ray source in a compact solar flare as evidence for magnetic reconnection. Nature **371**, 495–497 (1994). doi:10.1038/371495a0
14. Angelopoulos, V., Baumjohann, W., Kennel, C.F., Coronti, F.V., Kivelson, M.G., Pellat, R., Walker, R.J., Luehr, H., Paschmann, G.: Bursty bulk flows in the inner central plasma sheet. J. Geophys. Res. **97**, 4027–4039 (1992). doi:10.1029/91JA02701
15. Lui, A.T.Y., Mankofsky, A., Chang, C.L., Papadopoulos, K., Wu, C.S.: A current disruption mechanism in the neutral sheet – a possible trigger for substorm expansions. Geophys. Res. Lett. **17**, 745–748 (1990). doi:10.1029/GL017i006p00745
16. Sergeev, V., Angelopoulos, V., Apatenkov, S., Bonnell, J., Ergun, R., Nakamura, R., McFadden, J., Larson, D., Runov, A.: Kinetic structure of the sharp injection/dipolarization front in the flow-braking region. Geophys. Res. Lett. **36**, 21105 (2009). doi:10.1029/2009GL040658
17. Runov, A., Angelopoulos, V., Sitnov, M., Sergeev, V.A., Nakamura, R., Nishimura, Y., Frey, H.U., McFadden, J.P., Larson, D., Bonnell, J., Glassmeier, K.H., Auster, U., Connors, M., Russell, C.T., Singer, H.J.: Dipolarization fronts in the magnetotail plasma sheet. Planet. Space Sci. **59**, 517–525 (2011). doi:10.1016/j.pss.2010.06.006
18. Parker, E.N.: Magnetic neutral sheets in evolving fields - part two - formation of the solar corona. Astrophys. J. **264**, 642 (1983). doi:10.1086/160637
19. Phan, T.D., Gosling, J.T., Davis, M.S., Skoug, R.M., Øieroset, M., Lin, R.P., Lepping, R.P., McComas, D.J., Smith, C.W., Reme, H., Balogh, A.: A magnetic reconnection X-line extending more than 390 Earth radii in the solar wind. Nature **439**, 175–178 (2006). doi:10.1038/nature04393
20. Giacalone, J., Burgess, D.: Interaction between inclined current sheets and the heliospheric termination shock. Geophys. Res. Lett. **37**, 19104 (2010). doi:10.1029/2010GL044656
21. Retinò, A., Sundkvist, D., Vaivads, A., Mozer, F., André, M., Owen, C.J.: In situ evidence of magnetic reconnection in turbulent plasma. Nat. Phys. **3**, 236–238 (2007). doi:10.1038/nphys574
22. Runov, A., Baumjohann, W., Nakamura, R., Sergeev, V.A., Amm, O., Frey, H., Alexeev, I., Fazakerley, A.N., Owen, C.J., Lucek, E., André, M., Vaivads, A., Dandouras, I., Klecker, B.: Observations of an active thin current sheet. J. Geophys. Res. **113**, 7 (2008). doi:10.1029/2007JA012685

23. Chen, L.J., Bessho, N., Lefebvre, B., Vaith, H., Asnes, A., Santolik, O., Fazakerley, A., Puhl-Quinn, P., Bhattacharjee, A., Khotyaintsev, Y., Daly, P., Torbert, R.: Multispacecraft observations of the electron current sheet, neighboring magnetic islands, and electron acceleration during magnetotail reconnection. Phys. Plasma **16**(5), 056501 (2009). doi:10.1063/1.3112744
24. Vlahos, L., Krucker, S., Cargill, P.: The solar flare: a strongly turbulent particle accelerator. In: Lecture Notes in Physics, vol. 778, pp. 157 (2009). doi:10.1007/978-3-642-00210-6_5
25. Gosling, J.T.: Observations of magnetic reconnection in the turbulent high-speed solar wind. Astrophys. J. **671**, L73–L76 (2007). doi:10.1086/524842
26. Ji, H., Ren, Y., Yamada, M., Dorfman, S., Daughton, W., Gerhardt, S.P.: New insights into dissipation in the electron layer during magnetic reconnection. Geophys. Res. Lett. **35**, 13106 (2008). doi:10.1029/2008GL034538
27. Pritchett, P.L.: Energetic electron acceleration during multi-island coalescence. Phys. Plasma **15**(10), 102105 (2008). doi:10.1063/1.2996321
28. Daughton, W., Roytershteyn, V., Karimabadi, H., Yin, L., Albright, B.J., Bergen, B., Bowers, K.J.: Role of electron physics in the development of turbulent magnetic reconnection in collisionless plasmas. Nat. Phys. (2011). doi:10.1038/nphys1965
29. Shibata, K., Tanuma, S.: Plasmoid-induced-reconnection and fractal reconnection. Earth Planets Space **53**, 473–482 (2001)
30. Oka, M., Phan, T.-D., Krucker, S., Fujimoto, M., Shinohara, I.: Electron acceleration by multi-island coalescence. Astrophys. J. **714**, 915–926 (2010). doi:10.1088/0004-637X/714/1/915
31. Nakamura, T.K.M., Hasegawa, H., Shinohara, I., Fujimoto, M.: Evolution of an MHD-scale Kelvin-Helmholtz vortex accompanied by magnetic reconnection: two-dimensional particle simulations. J. Geophys. Res. **116**(A15), A03227 (2011). doi:10.1029/2010JA016046
32. Drake, J.F., Swisdak, M., Che, H., Shay, M.A.: Electron acceleration from contracting magnetic islands during reconnection. Nature **443**, 553–556 (2006). doi:10.1038/nature05116
33. Eastwood, J.P., Sibeck, D.G., Slavin, J.A., Goldstein, M.L., Lavraud, B., Sitnov, M., Imber, S., Balogh, A., Lucek, E.A., Dandouras, I.: Observations of multiple X-line structure in the Earth's magnetotail current sheet: a Cluster case study. Geophys. Res. Lett. **32**, 11105 (2005). doi:10.1029/2005GL022509
34. Chen, L.-J., Bhattacharjee, A., Puhl-Quinn, P.A., Yang, H., Bessho, N., Imada, S., Mühlbachler, S., Daly, P.W., Lefebvre, B., Khotyaintsev, Y., Vaivads, A., Fazakerley, A., Georgescu, E.: Observation of energetic electrons within magnetic islands. Nat. Phys. **4**, 19–23 (2008). doi:10.1038/nphys777
35. Retinò, A., Nakamura, R., Vaivads, A., Khotyaintsev, Y., Hayakawa, T., Tanaka, K., Kasahara, S., Fujimoto, M., Shinohara, I., Eastwood, J.P., André, M., Baumjohann, W., Daly, P.W., Kronberg, E.A., Cornilleau-Wehrlin, N.: Cluster observations of energetic electrons and electromagnetic fields within a reconnecting thin current sheet in the Earth's magnetotail. J. Geophys. Res. **113**, 12215 (2008). doi:10.1029/2008JA013511
36. Sreenivasan, K.: Turbulence and the tube. Nature **344**, 192 (1990)
37. Biskamp, D.: Magnetohydrodynamics Turbulence. Cambridge University Press, Cambridge, UK (2003)
38. Lazarian, A., Beresnyak, A., Yan, H., Opher, M., Liu, Y.: Properties and selected implications of magnetic turbulence for interstellar medium, local bubble and solar wind. Space Sci. Rev. **143**, 387–413 (2009). doi:10.1007/s11214-008-9452-y
39. Bruno, R., Carbone, V.: The Solar Wind as a Turbulence Laboratory. Living Rev. Sol. Phys. **2**, 4 (2005)
40. Brandenburg, A., Nordlund, A.: Astrophysical turbulence modeling. Rep. Prog. Phys. **74**(4), 046901 (2011). doi:10.1088/0034-4885/74/4/046901
41. Sorriso-Valvo, L., Yordanova, E., Carbone, V.: On the scaling properties of anisotropy of interplanetary magnetic turbulent fluctuations. Eur. Phys. Lett. **90**, 59001 (2010). doi:10.1209/0295-5075/90/59001
42. Goldreich, P., Sridhar, S.: Toward a theory of interstellar turbulence. 2: strong alfvenic turbulence. Astrophys. J. **438**, 763–775 (1995). doi:10.1086/175121
43. Horbury, T.S., Forman, M., Oughton, S.: Anisotropic scaling of magnetohydrodynamic turbulence. Phys. Rev. Lett. **101**(17), 175005 (2008). doi:10.1103/PhysRevLett.101.175005

44. Bieber, J.W., Wanner, W., Matthaeus, W.H.: Dominant two-dimensional solar wind turbulence with implications for cosmic ray transpor. J. Geophys. Res. **101**, 2511–2522 (1996). doi:10.1029/95JA02588
45. Narita, Y., Glassmeier, K.-H., Sahraoui, F., Goldstein, M.L.: Wave-vector dependence of magnetic-turbulence spectra in the solar wind. Phys. Rev. Lett. **104**(17), 171101 (2010). doi:10.1103/PhysRevLett.104.171101
46. Mininni, P.D., Alexakis, A., Pouquet, A.: Energy transfer in Hall-MHD turbulence: cascades, backscatter, and dynamo action. J. Plasma Phys. **73**, 377–401 (2007). doi:10.1017/S0022377806004624
47. Chen, C.H.K., Horbury, T.S., Schekochihin, A.A., Wicks, R.T., Alexandrova, O., Mitchell, J.: Anisotropy of solar wind turbulence between ion and electron scales. Phys. Rev. Lett. **104**(25), 255002 (2010). doi:10.1103/PhysRevLett.104.255002
48. Sahraoui, F., Goldstein, M.L., Belmont, G., Canu, P., Rezeau, L.: Three dimensional anisotropic k spectra of turbulence at subproton scales in the solar wind. Phys. Rev. Lett. **105**(13), 131101 (2010). doi:10.1103/PhysRevLett.105.131101
49. Cho, J., Lazarian, A.: Simulations of electron magnetohydrodynamic turbulence. Astrophys. J. **701**, 236–252 (2009). doi:10.1088/0004-637X/701/1/236
50. Sonnerup, B.U.Ö., Haaland, S., Paschmann, G.: Discontinuity Orientation, Motion and Thickness. ISSI SR-005, pp. 1–10 (2008)
51. Shi, Q.Q., Shen, C., Pu, Z.Y., Dunlop, M.W., Zong, Q.-G., Zhang, H., Xiao, C.J., Liu, Z.X., Balogh, A.: Dimensional analysis of observed structures using multipoint magnetic field measurements: application to cluster. Geophys. Res. Lett. **32**, 12105 (2005). doi:10.1029/2005GL022454
52. Shi, Q.Q., Shen, C., Dunlop, M.W., Pu, Z.Y., Zong, Q.-G., Liu, Z.X., Lucek, E., Balogh, A.: Motion of observed structures calculated from multi-point magnetic field measurements: application to cluster. Geophys. Res. Lett. **33**, 8109 (2006). doi:10.1029/2005GL025073
53. Harvey, C.C.: Spatial Gradients and the Volumetric Tensor. ISSI SR-001, p. 307 (1998)
54. CSDS: Cluster science data system. http://sci2.estec.esa.nl/cluster/csds/csds.html
55. AMDA: Automated multi-dataset analysis. cdpp-amda.cesr.fr/DDHTML/index.html